The NMDA receptor intracellular C-terminal domains reciprocally interact with allosteric modulators

Kiran Sapkota[1], Kim Dore[2], Kang Tang[1], Mark Irvine[3], Guangyu Fang[3], Erica S. Burnell[4], Roberto Malinow[2], David E. Jane[3*], Daniel T. Monaghan[1*#]

[1] Department of Pharmacology and Experimental Neuroscience, University of Nebraska Medical Center, Omaha, Nebraska 68198-5800 U.S.A.

[2] Center for Neural Circuits and Behavior, Department of Neuroscience and Section for Neurobiology, Division of Biology, University of California at San Diego, San Diego, CA, USA.

[3] Centre for Synaptic Plasticity, School of Physiology, Pharmacology & Neuroscience Biomedical Sciences Building,University Walk, University of Bristol, Bristol, BS8 1TD, UK.

[4] School of Chemistry, National University of Ireland Galway, Galway H91TK33, Ireland

* Contributed equally as senior authors

#Corresponding author:

Daniel T. Monaghan
Department of Pharmacology and Experimental Neuroscience
University of Nebraska Medical Center
Omaha, NE 68198-5800
1-402-559-7196, FAX: 1-402-559-7495
dtmonagh@unmc.edu

Abstract

N-Methyl-D-aspartate receptors (NMDARs) have multiple prominent roles in CNS function but their excessive or insufficient activity contributes to neuropathological/psychiatric disorders. Consequently, a variety of positive and negative allosteric modulators (PAMs and NAMs, respectively) have recently been developed. Although these modulators bind to extracellular domains, in the present report we find that the NMDAR's intracellular C-terminal domains (CTDs) significantly influence PAM/NAM activity. GluN2 CTD deletion robustly affected NAM and PAM activity with both enhancing and inhibiting effects that were compound-specific and NMDAR subunit-specific. In three cases, individual PAMs became NAMs at specific GluN2-truncated receptors. In contrast to GluN2, GluN1 CTD removal only reduced PAM activity of UBP684 and CIQ, and did not affect NAM activity. Consistent with these findings, agents altering phosphorylation state or intracellular calcium levels displayed receptor-specific and compound-specific effects on PAM activity. It is possible that the GluN2's M4 domain transmits intracellular modulatory signals from the CTD to the M1/M4 channel gating machinery and that this site is a point of convergence in the direct or indirect actions of several PAMs/NAMs thus rendering them sensitive to CTD status. Thus, allosteric modulators are likely to have a marked and varied sensitivity to post-translational modifications, protein-protein associations, and intracellular ions. The interaction between PAM activity and NMDAR CTDs appears reciprocal. GluN1 CTD-deletion eliminated UBP684, but not pregnenolone sulfate (PS), PAM activity. And, in the absence of agonists, UBP684, but not PS, was able to promote movement of fluorescently-tagged GluN1-CTDs. Thus, it may be possible to pharmacologically target NMDAR metabotropic activity in the absence of channel activation.

Keywords: N-methyl-D-aspartate, C-terminal domain, phosphorylation, allosteric modulators, desensitization, fluorescence resonance energy transfer

1. **Introduction**

N-methyl-D-aspartate receptors (NMDARs) are a family of ionotropic glutamate receptors activated by L-glutamate and glycine/D-serine [1-4]. NMDAR activation triggers multiple calcium-dependent intracellular responses that regulate various forms of synaptic plasticity and experience-dependent synaptogenesis. Behavioral experiments show that they are key for cognition and different forms of memory. However, excessive NMDAR activation causes neuronal cell death and may be a critical factor in stroke, traumatic brain injury and neurodegenerative diseases [5-7]. NMDAR hypofunction, on the other hand, is associated with CNS dysfunction and may underlie the symptoms of schizophrenia and cognitive impairment [8-11]. These findings have led to the development of a large number of NMDAR pharmacological agents over the past 35 years to provide neuroprotection in stroke, seizures, and neurodegenerative disorders. Unfortunately, clinical studies with these agents, for the most part, have been disappointing with limited therapeutic efficacy and unacceptable adverse effects [12].

Recently, several new classes of NMDAR allosteric modulators have been developed with new potential therapeutic applications. Relative to previously available pharmacological agents, these new compounds offer multiple advantages for therapeutic use, for reviews see [13-16]. For example, a NMDAR PAM, unlike an agonist, could enhance weak NMDAR signals in pathological conditions of NMDAR hypofunction without causing activation of other NMDARs that should stay inactive. However, there are incidental observations that the activity of some allosteric modulators can be lost or enhanced due to a change in the intracellular environment such as when whole cell recordings or outside-out patch recordings are generated [17-19]. Given the therapeutic potential of the allosteric modulators, it is important to understand the conditions in which these agents may gain or lose activity so that the appropriate receptor populations can be

targeted in disease. Also, clarifying the role of the CTD should provide a greater understanding of PAM and NAM mechanisms of action.

NMDAR complexes are composed of subunits from seven genes - GluN1, GluN2A-D, and GluN3A-B [20, 21]. These subunits assemble into hetero-tetrameric complexes in various combinations resulting in functionally-distinct NMDARs. The majority of NMDARs are thought to be composed of two glycine-binding GluN1 subunits and two glutamate-binding GluN2 subunits. Each subunit consists of an extracellular regulatory N-terminal domain (NTD), an extracellular ligand-binding domain (LBD) where glycine or L-glutamate bind (on GluN1 and GluN2, respectively), a transmembrane domain (TMD) consisting of 3 membrane-spanning segments (M1, M3, and M4) and one re-entrant loop (M2), and an intracellular C-terminal domain (CTD).

Although the CTD is not necessary for NMDAR function, *per se*, the NMDAR CTD is thought to be the primary means by which intracellular factors can modulate NMDAR function through its interactions with intracellular ions, post-translational modifications, and interacting proteins. The observations of altered PAM/NAM activity in cells with disturbed intracellular environments, suggest that the intracellular CTD could be influencing the activity of NAMs and PAMs. Thus, to determine the general effect of the CTD on allosteric modulator activity, we deleted the CTD from individual NMDAR subunits and evaluated NAM and PAM activity. GluN1 CTD-deletion of NMDARs expressed in *Xenopus laevis* oocytes affected only the PAMs UBP684 and CIQ. In contrast, GluN2 CTD-deletion had a marked effect on many allosteric modulators and these effects were highly specific to subunit subtype. Consistent with these findings, depleting intracellular calcium or altering basal phosphorylation state also modulated allosteric modulator activity in a compound-specific and subunit-specific manner. The interaction between CTDs and

allosteric modulator binding/activity appears to be reciprocal. Using fluorescently-tagged CTD NMDAR constructs expressed in hippocampal neurons, we find that UBP684, but not PS, can cause movement in the GluN1 CTD in the absence of agonists.

2. Methods and Materials

2.1 Compounds

GNE-8324 was kindly provided by Genentech (South San Francisco, CA, USA); MPX-004 and MPX-007 by Cadent Therapeutics (Cambridge, MA, USA). PYD-106 was purchased from Glixx Laboratories (Hopkinton, MA, USA), and DQP-1105 were purchased from Tocris-Bio-Techne (Minneapolis, MN, USA). TCN-201 and CIQ were purchased from HelloBio, (Bristol, England). UBP684 and UBP792 were from our own laboratories [22]. 5-Pregnen-3β-ol-20-onesulphate (pregnenolone sulfate, PS) and 5β-pregnan-3α-ol-20-onesulphate (pregnanolone sulphate, PAS) were purchased from Steraloids, Inc. (Newport, RI, USA). Stock solutions were prepared in DMSO and diluted to the desired concentration in recording buffer before each experiment. All other chemicals were obtained from Sigma-Aldrich (St. Louis, MO, USA).

2.2 GluN subunit RNA preparation

cDNA encoding the GluN1a was a generous gift of Dr. Shigetada Nakanishi (Kyoto, Japan) and cDNA encoding GluNA, GluN2C and GluN2D were kindly provided by Dr. Peter Seeburg (Heidelburg, Germany) and the GluN2B cDNA was the generous gift of Drs. Dolan Pritchett and David Lynch (Philadelphia, PA, USA). Plasmids were linearized with Not I (GluN1a), EcoR I (GluN2A, GluN2C and GluN2D) or Sal I (GluN2B) and transcribed *in vitro* with T3 (GluN2A, GluN2C), SP6 (GluN2B) or T7 (GluN1a, GluN2D) RNA polymerase using the mMessage

mMachine transcription kits (Ambion, Austin, TX, USA). C-terminal deletion was achieved by introducing a stop codon at 838K, 844K, 845Q, 855K and 869R of genes encoding GluN1a, GluN2A, GluN2B, GluN2C and GluN2D respectively and, hereafter, referred as GluN1$^{\Delta CTD}$, GluN2A$^{\Delta CTD}$, GluN2B$^{\Delta CTD}$, GluN2C$^{\Delta CTD}$ and GluN2D$^{\Delta CTD}$ respectively (see Fig. 1A). GluN1$^{\Delta CTD}$ was a kind gift from (Dr. Gary Westbrook, Portland, OR, USA). CTD-deleted constructs were verified by sequencing in the UNMC molecular core facility.

2.3 Oocyte preparations and GluN expression

Oocytes were removed and isolated from mature female *Xenopus* laevis (*Xenopus* One, Ann Arbor, MI, USA) as previously described [23] by procedures approved by the University of Nebraska Medical Center's Animal Care and Use Committee in compliance with National Institutes of Health guidelines. NMDAR subunit RNAs were dissolved in sterile distilled H_2O. GluN1a and GluN2 RNAs were mixed in a molar ratio of 1:3. 50 nl of the final RNA mixture was microinjected (15-30 ng total) into the cytoplasm of the oocyte. For expression of C-terminal deleted subunits, 10-20-fold more RNA, than wildtype, was injected to produce receptor responses of adequate size. Oocytes were incubated in ND-96 solution at 17 °C prior to electrophysiological assay (1-5 days).

2.4 Two-electrode voltage clamp (TEVC) electrophysiology

Electrophysiological responses were measured using a standard two-microelectrode voltage clamp amplifier (Warner Instruments, model OC-725B, Hamden, CT, USA) designed to provide fast clamp of large cells. The recording buffer contained 116 mM NaCl, 2 mM KCl, 0.3 mM

$BaCl_2$, 0.005 mM EDTA (or 0.01 mM DTPA), and 5 mM HEPES, pH 7.4. Response magnitude was determined by the steady plateau response elicited by bath application of 10 μM L-glutamate plus 10 μM glycine at a holding potential of –60 mV. Response amplitudes for the four heteromeric complexes were generally between 0.2 to 1.5 μA. In all experiments, control responses were obtained in parallel with experimental responses on the same batch of oocytes on the same day. The lack of significant activation of the endogenous Cl^- current by Ba^{2+} in these cells was indicated by the presence of a plateau response. After obtaining a steady-state response to agonist application, test compounds were bath applied by a 8- or 16-channel perfusion system (Automate Scientific, Berkeley, CA, USA) and the responses were digitized for quantification (Digidata 1440A and pClamp-10, Molecular Devices, San Jose, CA, USA). Dose-response relationships were fit to a single-site (GraphPad Prism, ISI Software, San Diego, CA, USA), using a nonlinear regression to calculate IC_{50} or EC_{50} and % maximal efficacy.

Especially for GluN2A-containing receptors, the magnitude of potentiation by different PAMs varied somewhat by oocyte batch (frog), days after RNA injection, and between different groups of frogs, but not as a function of agonist-response magnitude. Indeed, this variation was the initial motivation for the present study; competitive antagonists and channel blockers do not show such sensitivity. Thus, for all experiments, we used matched controls where full-length NMDAR responses were frequently alternated with experiments on CTD-deleted constructs on the same day and from the same batch of oocytes. Results shown represent averaged responses from oocytes from multiple frogs.

2.5 Oocyte cell-signaling treatments

For intracellular Ca^{2+} chelation, 5 mM EGTA was injected 1-2 h before recording. To study the effect of protein kinase C (PKC) mediated phosphorylation on PS and UBP684 activity, oocytes were bath superfused with 2 μM phorbol 12-myristate 13-acetate (PMA) for 10 minutes. Potentiation before and after PMA was calculated using the agonist response before and after PMA treatment. For de-phosphorylation of the receptors, oocytes were either microinjected with alkaline phosphatase (0.1 U/μL) and recorded 15-30 min post-injection or incubated in presence of the PKC inhibitor U73122 (20 μL) and recorded 30 min post treatment. For control experiments, the same volume of H_2O was microinjected.

2.6 CTD-FRET Studies

Rat primary hippocampal neurons were made according to previously described protocols with minor modifications [24]. Neurons were transfected at DIV 7-10 with ~2μg of total DNA (GluN1-GFP, GluN2A and GluN1-mCherry) and 4μL of Lipofectamine 2000 was used per well (18mm coverslips). Neurons expressing the desired constructs were imaged at 16-18DIV in a HBSS based solution containing: 0.87x HBSS, 5mM HEPES, 1mM Glucose, 2.5mM $MgCl_2$, 0.5mM $CaCl_2$. 75uM of UBP684 or PS were added to neurons after a baseline image was recorded, 10min after application of the test compound a second image was taken. Each neuron was imaged only twice and compounds were interleaved. Results are pooled from two different animal preparations. Fluorescence lifetime imaging was performed on a SliceScope two-photon microscope (Scientifica, UK) as previously described [24]. Briefly, a Chameleon Ultra II IR laser (Coherent, Santa Clara, CA, USA) tuned at 930 nm was used for the excitation (power was adjusted to 3mW after the microscope objective (LUMPLFLN 60XW, NA = 1.0, Olympus)). Fluorescence emission was detected with a hybrid PMT detector (HPM-100-40, Becker and Hickl, Germany) and synchronized by a TCSPC module (SPC-150, Becker and Hickl, Germany). The following parameters were kept constant

for all acquired images: pixel size (80 nm; all 512 × 512 pixels), pixel dwell time (3.2 μs), FLIM acquisition time (~120 s/image), and number of time bins (256) in the fluorescence decay curves. Fluorescence lifetime images were analyzed with SPCImage (Becker and Hickl, Germany) using a binning factor between 6 and 10 pixels, minimum threshold of 10 photons at the peak time bin, a single exponential model and used the same calculated instrumental response function for each set of experiments. For further analysis, each FLIM image was exported as a matrix of lifetimes, photon counts, and goodness of fit values (chi-squared) and analyzed blind to condition with a custom MATLAB script, see [24] for details.

2.7 Statistical analyses

All values are expressed as mean ± s.e.m. Paired and unpaired t-test were used for comparisons of two values; comparison of 3 or move values used a one-way ANOVA followed by Tukey's multiple comparisons test or a two-way ANOVA followed by Fisher's LSD test; $p < 0.05$ was considered as statistically significant.

3. Results

3.1 Both GluN1 and GluN2 NMDAR CTDs contribute to positive allosteric modulation by UBP684.

We have recently characterized the mechanism of action of the general NMDAR PAM, UBP684 [22, 25]. As this PAM can potentiate the activity of all four GluN1/GluN2A-D receptors, we used this compound to compare the effect of CTD-deletion at the different NMDAR subunits. Fig. 1A shows the truncation sites used for this study. UBP684 activity was significantly altered by deletion of the GluN2 subunit CTDs (Fig. 1C). Deletion of the GluN2A and GluN2D subunit

CTDs reduced the potentiation by UBP684 by approximately 50 % compared to wildtype. UBP684 (50 μM) potentiated GluN2A^{WT} receptors by 54 ± 7 % (n = 23 oocytes) and more weakly potentiated GluN2A$^{\Delta CTD}$ – containing receptors by 27 ± 5 % (n = 28 oocytes; $p<0.001$, two-way ANOVA). UBP684 potentiated GluN2D^{WT} receptors 50 ± 8 % (n = 11 oocytes) while only potentiating 23 ± 4 % (n = 13 oocytes) at receptors containing GluN2D$^{\Delta CTD}$ ($p<0.05$, two-way ANOVA). In contrast to the results with GluN2A and GluN2D subunits, UBP684 potentiation was enhanced when the GluN2B CTD was removed. UBP684 potentiation at GluN2B^{WT} and GluN2B$^{\Delta CTD}$ was 51 ± 6 % (n = 20 oocytes) and 74.4 ± 7.0 % (n = 15 oocytes), respectively ($p<0.01$, two-way ANOVA). Unexpectedly, UBP684 behaved as a NAM at GluN2C$^{\Delta CTD}$ subunit-containing receptors (Fig. 1B,C). UBP684 inhibited GluN2C$^{\Delta CTD}$ subunit-containing receptor responses by 20 ± 3 % (n = 12 oocytes) while potentiating GluN1/GluN2C^{WT} receptors by 58 ± 6 % (n = 15 oocytes; $p<0.0001$, two way ANOVA). Another distinct feature of the GluN2C-CTD-deleted receptor was that it displayed a slow desensitization not seen in the GluN1/GluN2C WT receptor.

To examine the role of the GluN1 CTD, GluN2A-D subunits were co-expressed with GluN1 with intact (GluN1^{WT}) or deleted (GluN1$^{\Delta CTD}$) CTDs. Although, GluN1 CTD deletion significantly reduced the potentiation at all GluN1/GluN2 receptors, its impact on GluN2A and GluN2C was more dramatic, essentially eliminating potentiating activity. UBP684 potentiation at GluN1$^{\Delta CTD}$/GluN2A, GluN1$^{\Delta CTD}$/GluN2B, GluN1$^{\Delta CTD}$/GluN2C and GluN1$^{\Delta CTD}$/GluN2D receptors was 3 ± 2 % (n = 17 oocytes), 44 ± 8 % (n = 6 oocytes), 5 ± 3 % (n = 6 oocytes) and 19 ± 7% (n = 14 oocytes), respectively while at experimentally-matched wildtype receptors, UBP684 potentiated GluN1/GluN2A: 39 ± 4 % (n = 22 oocytes), GluN1/GluN2B: 77 ± 7 % (n = 6 oocytes),

GluN1/GluN2C: 81 ± 7 % (n = 6 oocytes) and GluN1/GluN2D: 58 ± 6 % (n = 15 oocytes) (Fig. 1D).

The effects of CTD-deletion on NMDAR single channel activity is due to deletion of amino acids in the proximal region of the CTD nearest to M4 [26]. To determine which portion of the CTD is responsible for the deletion effects on UBP684 activity, we examined three constructs wherein the GluN2C -CTD was deleted at different positions, residue numbers 855, 994, and 1120; WT length is 1250 residues. Only the shortest construct, GluN2C-855KStop resulted in UBP684 having NAM activity at GluN2C; UBP684 activity in the longer constructs was similar to WT (Fig. 1E).

3.2 The CTDs of GluN2, but not GluN1 affect allosteric modulation by pregnenolone sulphate (PS).

The neurosteroid PS, an endogenous modulator of NMDARs, potentiates GluN2A- and GluN2B- containing receptors and inhibits GluN2C- and GluN2D-containing NMDARs [27-29]. As found for UBP684, deletion of the GluN2 CTD significantly altered PS PAM activity, but with qualitatively-distinct effects. Deletion of the GluN2A CTD resulted in PS displaying NAM activity at GluN2A (Fig. 2A,B). 100 μM PS potentiated GluN2A^{WT} receptors by 38 ± 4 % (n = 25 oocytes), whereas it inhibited GluN2A$^{\Delta CTD}$ - containing receptors by 23 ± 4 % (n = 25 oocytes; $p < 0.0001$, 2-way ANOVA). Removal of the CTD from GluN2B caused a partial reduction in PS PAM activity. PS potentiated GluN2B^{WT} receptors by 96 ± 6 %, n = 15 oocytes and GluN2B$^{\Delta CTD}$ receptors by 74 ± 10 %, n = 8 oocytes ($p < 0.05$, two-way ANOVA). Thus, the effect of GluN2B CTD-deletion had opposite effects on the actions of UBP684 and PS - enhancing UBP684 PAM activity while reducing PS PAM activity. Removal of the GluN2C CTD significantly increased PS

mediated inhibition (WT: 64 ± 4 % inhibition, n = 10 oocytes; CTD-deleted: 89 ± 2 %, n = 14 oocytes; $p<0.01$, two-way ANOVA). CTD deletion from GluN2D subunits did not change the inhibitory activity of PS (WT: 49 ± 1 %, n = 4 oocytes; CTD-deleted: 49 ± 8 %, n = 8 oocytes).

In contrast to the effects on UBP684 PAM activity, GluN1 subunit CTD-deletion did not reduce or eliminate PS PAM activity. GluN1 CTD deletion did not alter the PS activity at either GluN2A-, GluN2C- or GluN2D-containing receptors (GluN1/GluN2A: 33 ± 5 % potentiation, n = 24 oocytes; GluN1$^{\Delta CTD}$/GluN2A: 32 ± 4 % potentiation, n = 20 oocytes; GluN1/GluN2C: 81 ± 4 % inhibition, n = 6 oocytes; GluN1$^{\Delta CTD}$/GluN2C: 66 ± 5 % inhibition, n = 6 oocytes; GluN1/GluN2D: 43 ± 4 % inhibition (n = 12 oocytes) and GluN1$^{\Delta CTD}$/GluN2D: 45 ± 6 % inhibition (n = 14 oocytes). At GluN2B-containing receptors, incorporation of GluN1$^{\Delta CTD}$ subunits increased PS potentiation from 94 ± 4 (n = 6 oocytes) to 156 ± 25 % (n = 6 oocytes; $p<0.0001$, two-way ANOVA) (Fig. 2C). As found for UBP684, the effect of CTD-deletion on PS inhibition of GluN1/GluN2C was only found with removal of most of the C-terminal, suggesting that the residues critical to the effect of CTD-deletion are located in the initial, membrane-proximal portion of the CTD (Fig. 2D).

To better define the effect of GluN2 CTD-deletion on PS activity, we determined the dose-response properties of PS potentiation/inhibition at the four GluN1/GluN2$^{\Delta CTD}$ receptors (Fig. 3). GluN2A CTD-deletion converted PAM activity (GluN1/GluN2A WT potentiating EC_{50} = 42.1 ± 9.4) into NAM activity at all doses with the lowest being 3 μM. For GluN2B-containing receptors, lower doses of PS did not distinguish WT and CTD-deleted receptors but at the highest dose tested there appeared a reduced potentiation in the GluN1/ GluN2B$^{\Delta CTD}$ receptor, that was not

statistically-significant. The EC_{50} of PS for GluN2B was not affected by CTD-deletion (GluN2B WT, EC_{50} = 33.5 ± 13; GluN2B$^{\Delta CTD}$, EC_{50} = 29.6 ± 7.0).

CTD deletion from GluN2C increased the inhibitory potency of PS at GluN2C-containing receptors ten-fold. The IC_{50} for GluN2C-containing receptors with and without their CTD was 82.4 ± 16.3 μM and 7.8 ± 1.2 μM respectively (Fig. 3C). Similar, but weaker effects were seen by CTD-deletion at GluN2D receptors; PS two-fold more potently inhibited GluN2D$^{\Delta CTD}$ receptors (IC_{50} = 76.7 ± 19.1 %) than WT GluN1/GluN2D receptors (IC_{50} = 149.8 ± 18.0 %).

3.3 The GluN CTDs are critical for the activity of other PAMs

The differing effects of NMDAR subunit CTD-deletion on UBP684 and PS activity, led us to evaluate the impact of the CTDs on the activity of other known NMDAR PAMs with varied mechanisms of action and different binding sites. The effect of GluN2A CTD-deletion on the activity of the GluN2A-selective PAM GNE-8324, which binds in the inter-subunit LBD interface [30], was similar to that found for PS. The GluN2A CTD was necessary for the potentiating activity of GNE-8324 (Fig. 4A). 30 μM GNE-8324 potentiated wildtype GluN2A (GluN2A^{WT}) receptors by 35 ± 4 % (n = 26 oocytes) and inhibited the GluN2A CTD-deleted receptors (GluN2A$^{\Delta CTD}$) by 11 ± 2 % (n = 23 oocytes), $p<0.0001$, unpaired t- test). Spermine, which is a GluN2B-selective PAM that binds in the N-terminal domain [31-34], displayed significantly greater potentiation at GluN2B$^{\Delta CTD}$ receptors compared to GluN2B^{WT}-containing receptors (20 ± 3 % potentiation at GluN2B vs 57 ± 5 % GluN2B$^{\Delta CTD}$; Fig. 4B). The activity of PYD-106, a GluN2C-selective PAM that is thought to bind in the N-terminal domain/LBD interface of GluN2C subunits [35], was significantly decreased by GluN2C CTD-deletion (Fig. 4C). PYD-106 (30 μM) potentiated GluN2C^{WT} and GluN2C$^{\Delta CTD}$ receptors by 64 ± 4 % (n = 13 oocytes) and 21 ± 3 % (n = 9 oocytes)

respectively ($p < 0.0001$, unpaired t-test). Interestingly, however, deletion of the CTD's on GluN2C and GluN2D subunits did not have a significant effect on the potentiating activity of CIQ (Fig. 4D), a GluN2C/2D allosteric potentiator [36] whose actions require residues on M1 [37]. CIQ (10 μM) potentiated $GluN2C^{WT}$ receptors by 89 ± 8 % (n = 17 oocytes) and $GluN2C^{\Delta CTD}$ by 113 ± 13 % (n = 17 oocytes) and potentiated $GluN2D^{WT}$ receptors 72 ± 11 % (n = 7 oocytes) $GluN2D^{\Delta CTD}$ by 48 ± 5 % (n = 10 oocytes).

Given the robust effect of GluN1 CTD-deletion on UBP684, but not PS, we tested the $GluN1^{\Delta CTD}$ construct on the activity of a PAM affected by GluN2 CTD-deletion (GNE-8324) and a PAM unaffected by GluN2 CTD-deletion (CIQ). GNE-8324, like PS, was unaffected by GluN1 CTD deletion (Fig. 4E), whereas CIQ PAM activity was significantly reduced by GluN1 CTD-deletion (Fig. 4F). Using the GluN2C-selective PAM, PYD-106, we confirmed that the effect of GluN2 CTD-deletion on PAM activity was dependent upon removal of the membrane-proximal, and not the more distal, region of the CTD (Fig. 4G).

3.4 The GluN2 C-terminal modulates NMDAR inhibition by NAMs in a subunit-specific manner.

The widespread effect of C-terminal deletion on the potentiating activity of distinct classes of NMDAR PAMs suggests that the C-terminal may generally affect allosteric modulator activity. So, we tested a set of mechanistically-distinct NAMs on intact and CTD-deleted NMDARs. Since these agents have known binding sites, or known effects on single channel gating, their modulation by CTD-deletion may provide insights into how the CTD can interact with NAM mechanisms and channel gating. CTD-deletion increased the activity of the general NAM pregnanolone sulfate (PAS) on GluN2A-containing receptors (Fig. 5A). PAS (100 μM) inhibited $GluN2A^{WT}$ receptors

by 61 ± 3 % (n = 8 oocytes) and GluN1/GluN2A$^{\Delta CTD}$ receptors by 89 ± 2 % (n = 7 oocytes), $p<0.0001$, 2-way ANOVA. CTD deletion caused a smaller increase in PAS inhibition at GluN2B (GluN2B^{WT}: 67 ± 1 % (n = 3 oocytes); GluN2B$^{\Delta CTD}$: 76 ± 3 % (n = 4 oocytes), *$p<0.05$, two-way ANOVA. There was no significant effect of CTD removal from GluN2C and GluN2D receptors on PAS mediated inhibition. PAS inhibited 96 ± 1 % (n = 3 oocytes) at GluN2C and 93 ± 1 % (n = 3 oocytes) at GluN2C$^{\Delta CTD}$. PAS inhibited GluN2D containing wildtype receptors by 87 ± 2 % (n = 4 oocytes) and GluN2D$^{\Delta CTD}$ receptors by 85 ± 5 % (n = 3 oocytes).

The activity of another NAM, UBP792 [22], was similarly affected by GluN2 CTD-deletion in that the largest effects were to enhance inhibition at GluN1/GluN2A receptors. The GluN2A$^{\Delta CTD}$ receptor was inhibited 64 ± 6 % (n = 3 oocytes) by 30 μM UBP792, while the WT GluN2A-containing receptor was only inhibited by 22 ± 8 % (n = 4 oocytes). CTD-deletion of GluN2B and GluN2C subunits did not display a significant effect on UBP792 NAM activity. However, there was a slight reduction on UBP792 inhibitory activity at receptors with CTD-deleted GluN2D subunits (Fig. 5B). UBP792 inhibited wild-type GluN2D receptors by 86 ± 1 % (n = 3 oocytes) whereas it inhibited CTD-deleted GluN2D receptors by 68 ± 7 % (n = 4 oocytes; $p<0.05$, 2-way ANOVA). As found for PAS and UBP792, the GluN2C/D preferring NAM, DQP-1105 [19] displayed significantly greater activity at CTD-deleted GluN2A receptors (Fig. 5C). GluN2 CTD-deletion also appeared to increase DQP-1105 inhibition at GluN2C- and GluN2D-containing receptors, but only the effect on GluN1/GluN2C was statistically-significant. DQP-1105 (50 μM) inhibited GluN1/GluN2A receptors by 39 ± 3 % (n = 5 oocytes) and GluN1/GluN2A$^{\Delta CTD}$ receptors by 82 ± 4 % (n = 6 oocytes), $p<0.0001$, 2-way ANOVA. DQP-1105 (10 μM) inhibited GluN1/GluN2C receptors by 69 ± 2 % (n = 13 oocytes) and GluN1/GluN2C$^{\Delta CTD}$ receptors by 79 ± 4 % (n = 10 oocytes), $p<0.01$, 2-way ANOVA. The inhibition by DQP-1105 at

GluN2D^{WT} and GluN2D$^{\Delta CTD}$ -containing receptors was 87 ± 1 % (n = 3 oocytes) and 97 ± 2 % (n = 3 oocytes), respectively.

Given the strong effect that CTD-deletion has of enhancing NAM activity, particularly at GluN2A receptors, we tested three GluN2A-selective NAMs. These agents are known to bind within the LBD interface at the same location as the PAM GNE-8324, but with a differential effect on residues within the interface resulting in NAM rather than PAM activity [38]. In contrast to the other NAMs, we found that the inhibition by TCN-201, MPX-004 and MPX-007 [39, 40] were all significantly reduced, rather than increased, by GluN2A CTD-deletion. TCN-201 inhibited GluN2A^{WT} and GluN2A$^{\Delta CTD}$ receptors by 82 ± 2 % (n = 7 oocytes) and 53 ± 5 % (n = 8 oocytes; $p<0.05$, unpaired t-test) respectively (Fig. 5D). MPX-004 inhibited GluN2A^{WT} and GluN2A$^{\Delta CTD}$ -containing receptors by 75 ± 8 % (n = 3 oocytes) and 29 ± 13 % (n = 3 oocytes; $p < 0.05$, unpaired t-test) respectively (Fig. 5E). Similarly, MPX-007 inhibited GluN2A^{WT} and GluN2A$^{\Delta CTD}$-containing receptors by 77 ± 9 % (n = 3 oocytes) and 36 ± 6 % (n = 3 oocytes; $p < 0.05$, unpaired t-test) respectively (Fig. 5F). As found for PAMs, GluN2 CTD-deletion had a greater effect than deleting the GluN1 CTD on NAM activity. We did not observe any effect of GluN1 CTD-deletion on the activity of PAS, DQP-1105 and TCN-201 on GluN2A receptors (Fig. 5G-I).

3.5 Intracellular calcium levels can affect PAM activity at GluN1/GluN2A receptors.

A prominent role of the NMDAR CTD in PAM activity, particularly at GluN2A-containing receptors, is consistent with observations that dialysis of cells during whole cell recording or upon forming outside-out patches eliminates the PAM activity of PS and UBP684 [17, 18, 25] at GluN1/GluN2A receptors. Thus, soluble intracellular ions, phosphorylating/dephosphorylating

enzymes, or disrupted protein-protein interactions may account for loss of PAM activity in dialyzed cells. Since intracellular calcium can modulate NMDAR channel gating by CTD interactions with calcineurin and calmodulin [41-43], we evaluated the possible role of intracellular Ca^{++} on modulating PAM activity. UBP684 (50 μM) potentiated GluN1/GluN2A-GluN2D receptors in un-injected control oocytes and in control, H_2O-injected oocytes (Fig. 6). However, UBP684-mediated potentiation of GluN1/GluN2A receptors was mostly eliminated in oocytes injected with 5 mM EGTA (Fig. 6A) and partially reduced at GluN1/GluN2B receptors (Fig. 6B). UBP684 enhanced the agonist response at GluN1/GluN2A receptors by 54 ± 5 % (n = 17 oocytes) in un-injected control cells, by 47 ± 13 % (n = 7 oocytes) in H_2O-injected control cells and by only 9 ± 3 % (n = 19 oocytes) in EGTA-injected oocytes. For GluN1/GluN2B receptors, EGTA injection partially reduced UBP684 potentiation: UBP684-induced potentiation was 48 ± 4 % (n = 18 oocytes) for un-injected control, 45 ± 5 % (n = 15 oocytes) H_2O-injected control, and 28 ± 2 % (n = 22 oocytes) EGTA-injected oocytes. EGTA injection had no significant effect on UBP684 potentiation at GluN1/GluN2C or GluN1/GluN2D receptors (Fig. 6C, D) or PS potentiation at any of the NMDARs (Fig. 6E-H).

Both intracellular calcium levels and, as shown below, PKC can alter PAM activity. Since phospholipase C (PLC) leads to increases in intracellular cytoplasmic calcium and PKC activation, we tested if the PLC inhibitor U73122 (20 μM for 30 min.), would have an effect on PS/UBP684 PAM activity. We did not observe any significant change in UBP684 activity at receptors containing either GluN2A and GluN2B subunits (GluN2A: control, 24 ± 5 %, n = 15 oocytes; U73122-treated, 26 ± 4 %, n = 10 oocytes; GluN2B: control, 33 ± 4 %, n = 6 oocytes; U73122-treated, 29 ± 9 %, n = 4 oocytes) (Fig. 6I). However, PS potentiation was enhanced by 60 % at GluN2A receptors in U73122 treated oocytes whereas PS activity was not changed in U73122-

treated cells expressing GluN1/GluN2B receptors (Fig. 6J). PS potentiated GluN2A response from control cells by 45 ± 3 % (n = 16 oocytes) and U73122-treated cells by 105 ± 16 % (n = 12 oocytes) ($p<0.0001$, two-way ANOVA). PS potentiated GluN2B response from control cells by 82 ± 10 % (n = 6 oocytes) and U73122-treated cells by 98 ± 8 % (n = 7 oocytes).

3.6 Effect of phosphorylation state on potentiating activity of PS and UBP684

Another factor by which the CTDs are thought to modulate NMDAR channel function is through phosphorylation of residues either on the NMDAR CTD or on accessory proteins that may bind to the CTD or elsewhere on the NMDAR complex. Many studies have found a role for protein kinase A (PKA) and Ca^{++}-sensitive forms of PKC in modulating NMDAR activity (for reviews see [44-46]. Thus, we evaluated if increased PKA or PKC activity would alter PS or UBP684 PAM activity. PKA activation by forskolin (FSK) and prevention of dephosphorylation by 3-isobutyl-1-methylxanthine (IBMX) increased GluN1/GluN2A and GluN1/GluN2B mediated currents, especially in GluN2B expressing cells (Fig. 7A). However, the % potentiation by either UBP684 or PS was unchanged in these PKA-potentiated cells (Fig. 7B, C). As noted in the Methods and Materials section, the level of potentiation, especially at GluN1/GluN2A receptors sometimes varied between different groups of frogs. Hence we frequently tested responses in matched WT/control and CTD-deleted/treated oocytes on the same day and from oocytes from each frog in an alternating manner. The experiments in Fig. 7, using several different frogs from the same group, show a consistently reduced UBP684 PAM activity at GluN2A, but unchanged activity at GluN2B and unchanged PS activity (cf Fig. 1 and Fig. 7).

Activation of PKC by 2 μM PMA for 10 minutes increased agonist responses at GluN1/GluN2A and GluN1/GluN2B receptors as others have reported [47, 48] (Fig. 7D). UBP684 (50 μM) displayed a larger % potentiation after PMA exposure at both GluN2A- and GluN2B-containing receptors, although the increase in activity was only statistically-significant for GluN2B (Fig. 7E). Interestingly, deletion of the GluN2A or GluN2B CTDs did not eliminate the PMA-induced increase in UBP684 PAM activity, and indeed increased UBP684 PAM activity at GluN1/GluN2A (Fig. 7G). Since GluN2A CTD-deletion significantly reduces PAM activity, it is noteworthy that UBP684 PAM activity was restored by prior PMA exposure. Thus, the enhancement of UBP684 PAM activity by PMA is independent of the GluN2 CTD. As found for UBP684, PS PAM activity was significantly increased by PMA in the GluN2A CTD-deleted receptor, but not in the full-length receptor (Fig. 7F,H). Unlike UBP684, PS PAM activity at GluN2B receptors was unaffected by PMA (Fig. 7F). These results suggest that phosphorylation state, can affect PS/UPB684 PAM activity. However, the role of the GluN2 CTD is not simply to serve as a PKC substrate, since deleting the CTD can increase the PMA potentiating effect on UBP684/PS PAM activity. Since there was a statistically-significant effect of PMA on UBP684 potentiation on GluN1/GluN2B, but not on PS potentiation, we evaluated if alkaline phosphatase injections into oocytes would alter PAM activity. Phosphatase injection significantly reduced UBP684 potentiation, but not that of PS (Fig. 7I).

3.7 UBP684, but not PS, can cause movement of the GluN1 CTD.

The results of these studies indicate that removal of the NMDAR CTD, or changing the intracellular environment, can affect the activity of a mechanistically-diverse set of PAMs and NAMs in a highly compound-specific and subunit-specific manner. If the binding or function of

PAMs and NAMs is sensitive to the state of the CTD, then in a reciprocal manner, the CTD may be sensitive to the binding or action of PAMs and NAMs. Using methods previously described [24] we tested if PAMs can cause movement of the GluN1 CTD in rat hippocampal neurons expressing GluN1-GFP, GluN2A and GluN1-mCherry. Using a concentration for UBP684 and PS that is near the top of their dose response curves (EC_{50} ~ 30 μM for each), we find that 75 μM UBP684 caused a significant increase in GluN1-GFP fluorescence lifetime, which indicates a movement in the GluN1 CTD (Fig. 8). This movement went in the same direction as the one produced by the specific agonist NMDA [24], suggesting that UBP684 might have similar effects on GluN1 CTD conformation. In contrast to UBP684, application of 75 μM PS did not affect GluN1 CTD conformation (Fig. 8). These results are consistent with the finding that GluN1 CTD-deletion reduced UBP684 PAM activity but not that of PS at the GluN1/GluN2A receptor (Fig. 1, 2).

4. Discussion

4.1 CTD-deletion alters PAM/NAM activity and receptor subtype selectivity.

The results of the present study indicate that the activities of many allosteric modulators are significantly affected by the presence of NMDAR subunit CTDs in a manner that is highly compound-specific and receptor subunit-specific. As discussed below, these and other observations suggest that the effects of PAMs and NAMs may change markedly as a function of intracellular factors such as post-translational modifications (e.g. phosphorylation, palmitoylation, and ubiquitination), intracellular ion concentrations, and intracellular protein-protein interactions. Thus, it will be important to define the intracellular conditions that can affect CTD-modulation of

specific PAMs and NAMs so that the appropriate receptor population can be targeted if these agents are used therapeutically.

The effect of CTD-deletion on PAM/NAM activity is remarkable for both the extent and the specificity. CTD-deletion has little effect on NMDAR agonist potency and does not change channel blocker (memantine) activity or Zn^{++} modulation [49], but GluN2 CTD-deletion had many significant effects on allosteric modulator activity, especially on GluN1/GluN2A receptors. Upon GluN2A CTD-deletion, the PAMs PS and GNE-8324 become NAMs while UBP684 became a less effective PAM. NAMs were differentially affected; the structurally-diverse NAMs UBP792, PAS and DQP-1105 became stronger NAMs while the LBD interface-binding NAMs (TCN-201, MPX-004, MPX-007) become weaker NAMs. Compared to GluN2A, GluN2B CTD-deletion led to weaker changes in PAM/NAM activity and an increase of the PAM activity of UBP684 and spermine. GluN2C CTD-deletion mostly reduced potentiation and increased inhibition: CTD-deletion converted UBP684 PAM activity into inhibition, decreased PYD-106, but not CIQ potentiation, and increased PS and DQP-1105 inhibitory activity. Relative to GluN2C, GluN2D CTD-deletion had less effect on PAM/NAM activity: a reduction in UBP684 PAM activity, a minor increase in PS NAM potency, a minor reduction in UBP792 NAM activity, and no effect on the NAM activity of PAS, DQP-1105, or CIQ. In contrast to these varied effects of GluN2 CTD-deletion, the consequences of GluN1 CTD removal were more limited - an increase in PS potentiation specifically at $GluN1^{\Delta CTD}$/GluN2B receptors, a robust reduction in UBP684 PAM activity at all GluN1 CTD-deleted receptors, and a reduction in CIQ potentiation at $GluN1^{\Delta CTD}$/GluN2D receptors. GluN1 CTD-deletion did not affect GNE-8324 PAM activity or NAM activity of PS, PAS, TCN-201 or DQP-1105.

4.2 Potential convergence of PAM/NAM actions and CTD-derived signals at the M1/M4 peripheral ring.

The CTD may be affecting modulator activity through M4 which immediately precedes the CTD. Molecular dynamics simulations [50] and CTD-FRET [24] experiments suggest that the end of M4 nearest the CTD moves during activation. Thus, deleting the CTD may be affecting M4 movement during activation by altering the mobility or anchoring of the cytoplasmic end of the M4 helix. Consistent with this idea, mutating two palmitoylated GluN2A cysteine residues in the CTD located near M4 reduced the PAM activity of docoshexaenoic acid[51].

The significant effect of CTD-deletion on allosteric modulator activity, but relatively little effect on agonist and channel blocker activity might reflect that both the CTD and allosteric modulators can influence channel gating through interactions with the peripheral ring formed by the pre-M1, M1, and M4 helices that surround the central channel pore formed by M2/M3. The primary channel gating mechanism is thought be agonist-induced movement of M3 at the constriction formed by the four subunit's M3 helices near the extracellular surface of the membrane [52]. The surrounding ring formed by pre-M1, M1, and M4 appears to modulate channel gating and desensitization [53-56]. Thus, M4 is well positioned for transmitting intracellular signals from the CTD to modulate channel properties. As well-defined for some AMPA receptor NAMs [57], some NMDAR allosteric modulators are known to bind to, or require for their activity, residues in the pre-M1, M1 or M4 helices, for review see [13]. Other modulators such as spermine, PYD-106, PS, GNE-8324 may affect the M1/M4 peripheral ring via the S1/M1 or S2/M4 linkers. We cannot exclude, however, that the CTD could be interacting with M2 to affect channel gating properties, but in this case, one might expect a greater effect on the activity of open channel blockers.

4.3 The different effects of CTD-deletion of GluN1 and GluN2 subunits may reflect their different roles in channel gating and desensitization.

The greater impact of GluN2 CTD-deletion on allosteric modulator activity may reflect the divergent roles of GluN1 and GluN2 CTDs in modulating channel gating and desensitization. GluN1 CTD-deletion causes an increased unitary conductance, but does not affect open probability (Po), mean open time (MOT) or mean closed time (MCT) [26] but see [42]. In contrast, GluN2A or GluN2B CTD-deletion decreases Po [26, 58, 59] by increasing MCT [26] and desensitization [26, 60]. Similarly, crosslinking GluN2A M4 to the pre-M1 of the same subunit [53], or making GluN2 M4 point mutations [54-56] increases MCT and desensitization while the same modifications to GluN1 have only a minor effect. The biological relevance of GluN2 CTD modulation of desensitization is suggested by the decrease in desensitization upon GluN2 CTD association with PSD-95 [61] and the role of GluN2A/B-CTD phosphorylation in modulating NMDAR desensitization [60, 62, 63].

Since the GluN2 CTD can affect NMDAR desensitization state as a function of intracellular signals and protein binding partners, then allosteric modulators that also regulate desensitization state might be expected to interact cooperatively or antagonistically with the CTD signal regulating desensitization. Each of the NAMs PAS, UBP792, and DQP-1105 (or the simpler structural analogue 2-naphthoic acid in the case of UBP792) act to increase the long-lived closed states [19, 64, 65], and for each of these NAMs, GluN2A CTD-deletion enhanced their NAM activity. Thus, their inhibitory activity may further stabilize the long-lived closed states that are enhanced by CTD-deletion. The enhancement of NAM activity by facilitating the desensitized state is also consistent with DQP-1105's increased potency at GluN1/GluN2A receptors in a dialyzed whole cell recording mode [19], a condition which also promotes desensitization [66]. In contrast to the

NAMs PAS, UBP792, and DQP-1105, the three GluN2A NAMs that inhibit by binding in the LBD interdimer interface (TCN-201, MPX-004, MPX-007) were all less effective at the GluN2A-truncated receptor. The LBD interface-binding NAMs act by allosterically reducing glycine potency/occupancy [38, 39]. Since GluN2A CTD-deletion has been reported to increase glycine potency ~ 2-fold [49], some of the apparent loss of LBD-NAM activity may be due to increased glycine potency.

In the case of potentiators, enhancing the desensitized state (or long-lived closed states) by CTD-deletion may antagonize the activity of those PAMs, such as PS and UBP684, that act by reducing the long-lived closed states [17, 25]. This would account for the results found for PS and UBP684 which have reduced PAM activity at GluN1/GluN2A$^{\Delta CTD}$ receptors. Curiously, in three cases, GluN1/GluN2B receptors displayed enhanced PAM activity upon CTD-deletion; UBP684 and spermine displayed greater PAM activity upon GluN2B CTD-deletion while PS PAM activity was increased in the GluN1$^{\Delta CTD}$/GluN2B receptor. This suggests that the role of the CTD and/or M4 on desensitization mechanisms is quite different between receptors with GluN2A and GluN2B. In the case of Glu2C, we found that CTD-deletion promoted desensitization, enhanced NAM inhibitory activity and reduced PAM activity. Thus, as proposed for GluN2A CTD-deletion, promoting a desensitized state may further stabilize long-lived closed states and thus enhance NAM activity and reduce PAM activity.

Unlike PS and UBP684, the PAM activity of CIQ was mostly unaffected by GluN2 CTD-deletion and, like UBP684 (and unlike PS), was affected by GluN1 CTD-deletion. This may reflect that the binding site of CIQ appears to involve GluN2 M1/pre-M1 residues that are more closely associated with GluN1's M4 than with GluN2's M4 [37]. This is consistent with the identification

of residues at the extracellular end of GluN1's M4 that affect CIQ activity [37] and UBP684 PAM activity [13].

4.4 Intracellular modulation of PAM/NAM activity

Our brief evaluation of second messenger effects on PAM/NAM activity also suggests a role of the CTDs in affecting allosteric modulator activity. As found for CTD-deletion, modulation of PKC, PLC, phosphatase activity and intracellular calcium levels markedly affected allosteric modulator activity often affecting UBP684 and PS differently and distinguishing between receptor subtypes. At GluN1/GluN2B receptors, PMA increased UBP684 PAM activity but not that of PS and conversely, phosphatase injections reduced UBP684 but not PS PAM activity. This enhancement was still present after deleting the GluN2B CTD. In contrast, PKA activation did not change either UBP684 or PS potentiation even though PKA activation was able to increase agonist-induced WT NMDAR responses. It has been reported that PKA mediated phosphorylation is necessary for PS PAM activity [18], it could be that in the present studies, the basal level of PKA phosphorylation supports PS (and UBP684) PAM activity and it is only with a disrupted intracellular environment, as in outside-out patches, that there is dephosphorylation at PKA sites (and protein-protein disruption) which causes a reduction in PS PAM activity [18].

PLC inhibition and chelation of intracellular calcium chelation also had differential effects on PAM activity. EGTA injections significantly reduced UBP684 potentiation at GluN2A and GluN2B-containing receptors but not at those with GluN2C or GluN2D subunits; EGTA did not reduce PS potentiation at any receptor. Perhaps the interaction of calcium binding proteins with the GluN1 C-terminal [42] can affect UBP684 potentiation which is dependent on the GluN1 CTD

whereas PS potentiation is not. The calmodulin binding site on the GluN2A proximal CTD [43] may also contribute to calcium modulation of PAM activity. In addition to phosphorylation, palmitoylation of membrane-proximal CTD cysteine residues on GluN2A and GluN2B [67] might alter PAM/NAM activity as mutating these residues reduced PAM activity of docosahexaenoic acid on GluN1/GluN2A [51]. However, since these palmitoylated cysteines are conserved between GluN2A and GluN2B and absent from GluN1, these sites cannot fully account for the varied effects of CTD-deletion of GluN1, GluN2A and GluN2B subunits.

4.5 Reciprocal modulation of GluN1 CTD mobility by UBP684, but not by PS

By definition, allosteric modulators do not activate NMDAR channels as do agonists. However, the observation that the status of the CTD can allosterically affect the activity of both PAMs and NAMs, suggests that in a reciprocal manner, allosteric modulators can potentially modulate the CTD independent of channel activation. Recent studies have shown that agonists can alter the relative position of the GluN1 CTD in an NMDAR complex, providing a mechanism for a metabotropic-like action of NMDAR activation [24]. In this study, we found that UBP684, but not PS, was able to modify the relative position of the two GluN1 CTDs. This is consistent with a reciprocal interaction between the CTD and the allosteric modulator since GluN1 CTD-deletion reduced UBP684, but not PS, PAM activity. Consequently, some allosteric modulators may have the ability to modulate NMDAR metabotropic activity independent of agonist-induced channel activation.

4.6 Implications of the findings

There are several implications of these findings. CTD-deleted receptors [26, 60] are similar to PSD-95-dissociated NMDARs [61] in having greater desensitization. Thus, extrasynaptic NMDARs, if not associated with a PDZ-binding scaffold protein, may have a markedly different allosteric modulator pharmacology than the synaptic NMDARs. Since extrasynaptic receptors are thought to preferentially contribute to excitotoxicity and cell death [68], then it may be possible to target pathogenic NMDARs. As such, LBD-interface NAMs may potentially be relatively ineffective in providing neuroprotection while the desensitization-promoting NAMs may be especially-effective neuroprotective agents. In a similar manner, neuronal systems that have experienced PKA/PKC signals, such as with mGluR signaling, may have a modified NMDAR PAM/NAM pharmacology. These results also suggest that drug screening for allosteric modulators using recombinant receptors expressed in heterologous expression systems may yield biased results favoring receptors in specific post-translational states or unknown scaffold-bound states.

Another implication of the current study is that CTD-deletion may well alter the specific relationships between M4 / pre-M1 / and M3 in the resting state and alter the structural response to allosteric modulator binding. In three cases we found that CTD-deletion converted a PAM into a NAM. Hence, structural studies (crystallography, cryo-EM, molecular dynamics simulations) of CTD-deleted structures with these PAMs might reflect a relatively inactive state when the PAM is bound rather than a potentiated state.

The recent development of many new classes of NMDAR positive and negative allosteric modulators represents new potential opportunities for therapeutic treatment of many neurological/psychiatric disorders [13, 15, 16, 69]. The results from the present study suggest that the activity of these agents is likely to be quite sensitive to a variety of cellular factors –

phosphorylation, palmitoylation, ubiquitination, intracellular ion concentrations, and intracellular protein-protein interactions. Furthermore, since NMDAR activation can alter each of these factors [67, 70-72], repetitive receptor activation, as in epilepsy, could alter PAM/NAM activity. Thus, allosteric modulators represent new possibilities, but with distinct challenges, for targeting specific subpopulations of NMDAR receptors such as those in different states of second messenger regulation or coupling to scaffold proteins. These agents may also allow for independently targeting the ionotropic and metabotropic actions of NMDARs.

Acknowledgements:

This work was supported by the National Institutes of Mental Health (Grant MH60252) and Biotechnology and Biological Sciences Research Council (grant BB/L001977/1). We gratefully acknowledge Drs. Shigetada Nakanishi, Peter Seeburg, Dolan Pritchett David Lynch, and Gary Westbrook for providing cDNA constructs used in this study.

The authors note that they have no conflicts of interest.

References

[1] D.T. Monaghan, R.J. Bridges, C.W. Cotman, The excitatory amino acid receptors: their classes, pharmacology, and distinct properties in the function of the central nervous system, Annual Review of Pharmacology and Toxicology 29(1) (1989) 365-402.

[2] S.F. Traynelis, L.P. Wollmuth, C.J. McBain, F.S. Menniti, K.M. Vance, K.K. Ogden, K.B. Hansen, H. Yuan, S.J. Myers, R. Dingledine, Glutamate receptor ion channels: structure, regulation, and function, Pharmacological Reviews 62(3) (2010) 405-496.

[3] R. Dingledine, K. Borges, D. Bowie, S.F. Traynelis, The glutamate receptor ion channels, Pharmacological Reviews 51(1) (1999) 7-62.

[4] J.C. Watkins, D.E. Jane, The glutamate story, Br J Pharmacol 147 Suppl 1 (2006) S100-8.

[5] I. Mody, J.F. MacDonald, NMDA receptor-dependent excitotoxicity: the role of intracellular Ca2+ release, Trends Pharmacol Sci 16(10) (1995) 356-9.

[6] D.W. Choi, J.Y. Koh, S. Peters, Pharmacology of glutamate neurotoxicity in cortical cell culture: attenuation by NMDA antagonists, J Neurosci 8(1) (1988) 185-96.

[7] E. Koutsilieri, P. Riederer, Excitotoxicity and new antiglutamatergic strategies in Parkinson's disease and Alzheimer's disease, Parkinsonism Relat Disord 13 Suppl 3 (2007) S329-31.

[8] J.T. Coyle, G. Tsai, D. Goff, Converging evidence of NMDA receptor hypofunction in the pathophysiology of schizophrenia, Annals of the New York Academy of Sciences 1003(1) (2003) 318-327.

[9] J.E. Lisman, J.T. Coyle, R.W. Green, D.C. Javitt, F.M. Benes, S. Heckers, A.A. Grace, Circuit-based framework for understanding neurotransmitter and risk gene interactions in schizophrenia, Trends in neurosciences 31(5) (2008) 234-242.

[10] J.T. Kantrowitz, D.C. Javitt, Thinking glutamatergically: changing concepts of schizophrenia based upon changing neurochemical models, Clinical Schizophrenia & Related Psychoses 4(3) (2010) 189-200.

[11] K. Sapkota, Z. Mao, P. Synowicki, D. Lieber, M. Liu, T. Ikezu, V. Gautam, D.T. Monaghan, GluN2D N-Methyl-d-Aspartate Receptor Subunit Contribution to the Stimulation of Brain Activity and Gamma Oscillations by Ketamine: Implications for Schizophrenia, The Journal of Pharmacology and Experimental Therapeutics 356(3) (2016) 702-711.

[12] L.V. Kalia, S.K. Kalia, M.W. Salter, NMDA receptors in clinical neurology: excitatory times ahead, The Lancet Neurology 7(8) (2008) 742-755.

[13] E.S. Burnell, M. Irvine, G. Fang, K. Sapkota, D.E. Jane, D.T. Monaghan, Positive and Negative Allosteric Modulators of N-Methyl-d-aspartate (NMDA) Receptors: Structure–Activity Relationships and Mechanisms of Action, Journal of medicinal chemistry (2018).

[14] K.K. Ogden, S.F. Traynelis, New advances in NMDA receptor pharmacology, Trends in pharmacological sciences 32(12) (2011) 726-733.

[15] D.T. Monaghan, M.W. Irvine, B.M. Costa, G. Fang, D.E. Jane, Pharmacological modulation of NMDA receptor activity and the advent of negative and positive allosteric modulators, Neurochemistry International 61(4) (2012) 581-592.

[16] G.L. Collingridge, A. Volianskis, N. Bannister, G. France, L. Hanna, M. Mercier, P. Tidball, G. Fang, M.W. Irvine, B.M. Costa, The NMDA receptor as a target for cognitive enhancement, Neuropharmacology 64 (2013) 13-26.

[17] D.A. Chopra, D.T. Monaghan, S.M. Dravid, Bidirectional Effect of Pregnenolone Sulfate on GluN1/GluN2A N-Methyl-D-Aspartate Receptor Gating Depending on Extracellular Calcium and Intracellular Milieu, Molecular Pharmacology 88(4) (2015) 650-659.

[18] M. Petrovic, M. Sedlacek, O. Cais, M. Horak, H. Chodounska, L. Vyklicky, Pregnenolone sulfate modulation of N-methyl-D-aspartate receptors is phosphorylation dependent, Neuroscience 160(3) (2009) 616-628.

[19] T.M. Acker, H. Yuan, K.B. Hansen, K.M. Vance, K.K. Ogden, H.S. Jensen, P.B. Burger, P. Mullasseril, J.P. Snyder, D.C. Liotta, S.F. Traynelis, Mechanism for noncompetitive inhibition by novel

GluN2C/D N-methyl-D-aspartate receptor subunit-selective modulators, Molecular Pharmacology 80(5) (2011) 782-795.

[20] M.L. Mayer, N. Armstrong, Structure and function of glutamate receptor ion channels, Annu. Rev. Physiol. 66 (2004) 161-181.

[21] P. Paoletti, J. Neyton, NMDA receptor subunits: function and pharmacology, Current opinion in pharmacology 7(1) (2007) 39-47.

[22] K. Sapkota, M.W. Irvine, G. Fang, E.S. Burnell, N. Bannister, A. Volianskis, G.R. Culley, S.M. Dravid, G.L. Collingridge, D.E. Jane, Mechanism and properties of positive allosteric modulation of N-methyl-D-aspartate receptors by 6-alkyl 2-naphthoic acid derivatives, Neuropharmacology 125 (2017) 64-79.

[23] A.L. Buller, H.C. Larson, B.E. Schneider, J.A. Beaton, R.A. Morrisett, D.T. Monaghan, The molecular basis of NMDA receptor subtypes: native receptor diversity is predicted by subunit composition, The Journal of Neuroscience 14(9) (1994) 5471-5484.

[24] K. Dore, J. Aow, R. Malinow, Agonist binding to the NMDA receptor drives movement of its cytoplasmic domain without ion flow, Proceedings of the National Academy of Sciences of the United States of America 112(47) (2015) 14705-14710.

[25] D.A. Chopra, K. Sapkota, M.W. Irvine, G. Fang, D.E. Jane, D.T. Monaghan, S.M. Dravid, A single-channel mechanism for pharmacological potentiation of GluN1/GluN2A NMDA receptors, Scientific reports 7(1) (2017) 6933.

[26] B.A. Maki, T.K. Aman, S.A. Amico-Ruvio, C.L. Kussius, G.K. Popescu, C-terminal domains of N-methyl-D-aspartic acid receptor modulate unitary channel conductance and gating, The Journal of Biological Chemistry 287(43) (2012) 36071-36080.

[27] M.D. Majewska, R.D. Schwartz, Pregnenolone-sulfate: an endogenous antagonist of the γ-aminobutyric acid receptor complex in brain?, Brain research 404(1-2) (1987) 355-360.

[28] A. Malayev, T.T. Gibbs, D.H. Farb, Inhibition of the NMDA response by pregnenolone sulphate reveals subtype selective modulation of NMDA receptors by sulphated steroids, British Journal of Pharmacology 135(4) (2002) 901-909.

[29] M. Horak, K. Vlcek, H. Chodounska, L. Vyklicky, Subtype-dependence of N-methyl-D-aspartate receptor modulation by pregnenolone sulfate, Neuroscience 137(1) (2006) 93-102.

[30] D.H. Hackos, P.J. Lupardus, T. Grand, Y. Chen, T.-M. Wang, P. Reynen, A. Gustafson, H.J.A. Wallweber, M. Volgraf, B.D. Sellers, Positive allosteric modulators of GluN2A-containing NMDARs with distinct modes of action and impacts on circuit function, Neuron 89(5) (2016) 983-999.

[31] J. Lerma, Spermine regulates N-methyl-D-aspartate receptor desensitization, Neuron 8(2) (1992) 343-352.

[32] J.F. McGurk, M.V. Bennett, R.S. Zukin, Polyamines potentiate responses of N-methyl-D-aspartate receptors expressed in xenopus oocytes, Proceedings of the National Academy of Sciences of the United States of America 87(24) (1990) 9971-9974.

[33] D.J. Huggins, G.H. Grant, The function of the amino terminal domain in NMDA receptor modulation, Journal of Molecular Graphics and Modelling 23(4) (2005) 381-388.

[34] J.N. Kew, J.A. Kemp, An allosteric interaction between the NMDA receptor polyamine and ifenprodil sites in rat cultured cortical neurones, The Journal of Physiology 512(1) (1998) 17-28.

[35] A. Khatri, P.B. Burger, S.A. Swanger, K.B. Hansen, S. Zimmerman, E. Karakas, D.C. Liotta, H. Furukawa, J.P. Snyder, S.F. Traynelis, Structural determinants and mechanism of action of a GluN2C-selective NMDA receptor positive allosteric modulator, Molecular Pharmacology 86(5) (2014) 548-560.

[36] P. Mullasseril, K.B. Hansen, K.M. Vance, K.K. Ogden, H. Yuan, N.L. Kurtkaya, R. Santangelo, A.G. Orr, P. Le, K.M. Vellano, A subunit-selective potentiator of NR2C-and NR2D-containing NMDA receptors, Nature Communications 1 (2010) 90.

[37] K.K. Ogden, S.F. Traynelis, Contribution of the M1 transmembrane helix and pre-M1 region to positive allosteric modulation and gating of N-methyl-D-aspartate receptors, Molecular Pharmacology 83(5) (2013) 1045-1056.

[38] F. Yi, T.-C. Mou, K.N. Dorsett, R.A. Volkmann, F.S. Menniti, S.R. Sprang, K.B. Hansen, Structural Basis for Negative Allosteric Modulation of GluN2A-Containing NMDA Receptors, Neuron 91(6) (2016) 1316-1329.

[39] E. Bettini, A. Sava, C. Griffante, C. Carignani, A. Buson, A.M. Capelli, M. Negri, F. Andreetta, S.A. Senar-Sancho, L. Guiral, F. Cardullo, Identification and characterization of novel NMDA receptor antagonists selective for NR2A- over NR2B-containing receptors, The Journal of Pharmacology and Experimental Therapeutics 335(3) (2010) 636-644.

[40] R.A. Volkmann, C.M. Fanger, D.R. Anderson, V.R. Sirivolu, K. Paschetto, E. Gordon, C. Virginio, M. Gleyzes, B. Buisson, E. Steidl, MPX-004 and MPX-007: New Pharmacological Tools to Study the Physiology of NMDA Receptors Containing the GluN2A Subunit, PloS One 11(2) (2016) e0148129.

[41] M.D. Ehlers, S. Zhang, J.P. Bernhardt, R.L. Huganir, Inactivation of NMDA receptors by direct interaction of calmodulin with the NR1 subunit, Cell 84(5) (1996) 745-755.

[42] J.J. Krupp, B. Vissel, C.G. Thomas, S.F. Heinemann, G.L. Westbrook, Interactions of calmodulin and alpha-actinin with the NR1 subunit modulate Ca2+-dependent inactivation of NMDA receptors, The Journal of Neuroscience 19(4) (1999) 1165-1178.

[43] G. Bajaj, A.M. Hau, P. Hsu, P.R. Gafken, M.I. Schimerlik, J.E. Ishmael, Identification of an atypical calcium-dependent calmodulin binding site on the C-terminal domain of GluN2A, Biochem Biophys Res Commun 444(4) (2014) 588-94.

[44] M.P. Lussier, A. Sanz-Clemente, K.W. Roche, Dynamic regulation of N-Methyl-d-aspartate (NMDA) and α-Amino-3-hydroxy-5-methyl-4-isoxazolepropionic acid (AMPA) receptors by posttranslational modifications, Journal of Biological Chemistry 290(48) (2015) 28596-28603.

[45] B.-S. Chen, K.W. Roche, Regulation of NMDA receptors by phosphorylation, Neuropharmacology 53(3) (2007) 362-368.

[46] J.Q. Wang, M.-L. Guo, D.-Z. Jin, B. Xue, E.E. Fibuch, L.-M. Mao, Roles of subunit phosphorylation in regulating glutamate receptor function, European Journal of Pharmacology 728 (2014) 183-187.

[47] Y. Lin, T. Jover-Mengual, J. Wong, M.V. Bennett, R.S. Zukin, PSD-95 and PKC converge in regulating NMDA receptor trafficking and gating, Proceedings of the National Academy of Sciences 103(52) (2006) 19902-19907.

[48] E. Sigel, R. Baur, P. Malherbe, Protein kinase C transiently activated heteromeric N-methyl-D-aspartate receptor channels independent of the phosphorylatable C-terminal splice domain and of consensus phosphorylation sites, The Journal of biological chemistry 269(11) (1994) 8204-8208.

[49] C.A. Puddifoot, P.E. Chen, R. Schoepfer, D.J.A. Wyllie, Pharmacological characterization of recombinant NR1/NR2A NMDA receptors with truncated and deleted carboxy termini expressed in Xenopus laevis oocytes, British journal of pharmacology 156(3) (2009) 509-518.

[50] W. Zheng, H. Wen, G.J. Iacobucci, G.K. Popescu, Probing the structural dynamics of the NMDA receptor activation by coarse-grained modeling, Biophysical journal 112(12) (2017) 2589-2601.

[51] T.J. Wilding, M.N. Lopez, J.E. Huettner, Chimeric Glutamate Receptor Subunits Reveal the Transmembrane Domain Is Sufficient for NMDA Receptor Pore Properties but Some Positive Allosteric Modulators Require Additional Domains, The Journal of neuroscience : the official journal of the Society for Neuroscience 36(34) (2016) 8815-8825.

[52] E.C. Twomey, A.I. Sobolevsky, Structural Mechanisms of Gating in Ionotropic Glutamate Receptors, Biochemistry 57(3) (2018) 267-276.

[53] R. Kazi, Q. Gan, I. Talukder, M. Markowitz, C.L. Salussolia, L.P. Wollmuth, Asynchronous movements prior to pore opening in NMDA receptors, The Journal of Neuroscience 33(29) (2013) 12052-12066.

[54] J.B. Amin, C.L. Salussolia, K. Chan, M.C. Regan, J. Dai, H.-X. Zhou, H. Furukawa, M.E. Bowen, L.P. Wollmuth, Divergent roles of a peripheral transmembrane segment in AMPA and NMDA receptors, The Journal of general physiology (2017) jgp. 201711762.

[55] H. Ren, Y. Zhao, D.S. Dwyer, R.W. Peoples, Interactions among positions in the third and fourth Membrane-associated domains at the intersubunit interface mf the N-Methyl-D-Aspartate Receptor Forming Sites of alcohol action, Journal of Biological Chemistry (2012) jbc. M111. 338921.

[56] Y. Zhao, H. Ren, R. Peoples, Intersubunit interactions at putative sites of ethanol action in the M3 and M4 domains of the NMDA receptor GluN1 and GluN2B subunits, British journal of pharmacology 173(12) (2016) 1950-1965.

[57] M.V. Yelshanskaya, A.K. Singh, J.M. Sampson, C. Narangoda, M. Kurnikova, A.I. Sobolevsky, Structural bases of noncompetitive inhibition of AMPA-subtype ionotropic glutamate receptors by antiepileptic drugs, Neuron 91(6) (2016) 1305-1315.

[58] P. Punnakkal, P. Jendritza, G. Köhr, Influence of the intracellular GluN2 C-terminal domain on NMDA receptor function, Neuropharmacology 62(5) (2012) 1985-1992.

[59] R. Mohrmann, G. Köhr, H. Hatt, R. Sprengel, K. Gottmann, Deletion of the C-terminal domain of the NR2B subunit alters channel properties and synaptic targeting of N-methyl-D-aspartate receptors in nascent neocortical synapses, Journal of Neuroscience Research 68(3) (2002) 265-275.

[60] J.J. Krupp, B. Vissel, C.G. Thomas, S.F. Heinemann, G.L. Westbrook, Calcineurin acts via the C-terminus of NR2A to modulate desensitization of NMDA receptors, Neuropharmacology 42(5) (2002) 593-602.

[61] L. Sornarajah, O.C. Vasuta, L. Zhang, C. Sutton, B. Li, A. El-Husseini, L.A. Raymond, NMDA receptor desensitization regulated by direct binding to PDZ1-2 domains of PSD-95, Journal of neurophysiology 99(6) (2008) 3052-3062.

[62] T.K. Aman, B.A. Maki, T.J. Ruffino, E.M. Kasperek, G.K. Popescu, Separate intramolecular targets for protein kinase A control N-methyl-D-aspartate receptor gating and Ca2+ permeability, The Journal of biological chemistry 289(27) (2014) 18805-18817.

[63] B.A. Maki, R. Cole, G.K. Popescu, Two serine residues on GluN2A C-terminal tails control NMDA receptor current decay times, Channels 7(2) (2013) 126-132.

[64] C.L. Kussius, N. Kaur, G.K. Popescu, Pregnanolone sulfate promotes desensitization of activated NMDA receptors, The Journal of Neuroscience 29(21) (2009) 6819-6827.

[65] H. Yu, G.K. Popescu, Inhibition of GluN2A-containing N-methyl-D-aspartate receptors by 2-naphthoic acid, Molecular pharmacology 84(4) (2013) 541-550.

[66] B. Li, Y. Otsu, T.H. Murphy, L.A. Raymond, Developmental decrease in NMDA receptor desensitization associated with shift to synapse and interaction with postsynaptic density-95, Journal of Neuroscience 23(35) (2003) 11244-11254.

[67] T. Hayashi, G.M. Thomas, R.L. Huganir, Dual palmitoylation of NR2 subunits regulates NMDA receptor trafficking, Neuron 64(2) (2009) 213-226.

[68] G.E. Hardingham, H. Bading, Synaptic versus extrasynaptic NMDA receptor signalling: implications for neurodegenerative disorders, Nature Reviews Neuroscience 11(10) (2010) 682.

[69] K.B. Hansen, F. Yi, R.E. Perszyk, H. Furukawa, L.P. Wollmuth, A.J. Gibb, S.F. Traynelis, Structure, function, and allosteric modulation of NMDA receptors, J Gen Physiol 150(8) (2018) 1081-1105.

[70] P. Steiner, M.J. Higley, W. Xu, B.L. Czervionke, R.C. Malenka, B.L. Sabatini, Destabilization of the postsynaptic density by PSD-95 serine 73 phosphorylation inhibits spine growth and synaptic plasticity, Neuron 60(5) (2008) 788-802.

[71] B. Vissel, J.J. Krupp, S.F. Heinemann, G.L. Westbrook, A use-dependent tyrosine dephosphorylation of NMDA receptors is independent of ion flux, Nat Neurosci 4(6) (2001) 587-96.

[72] K. Dore, S. Labrecque, C. Tardif, P. De Koninck, FRET-FLIM investigation of PSD95-NMDA receptor interaction in dendritic spines; control by calpain, CaMKII and Src family kinase, PLoS One 9(11) (2014) e112170.

Figure legends:

Figure 1. Effect of NMDAR C-terminals on positive allosteric modulation by UBP684

(**A**) Left: Two-dimensional representation of a single NMDAR subunit showing four domains: extracellular N-terminal domain (NTD), ligand-binding domain (LBD), transmembrane domain (TMD) and intracellular C-terminal domain (CTD). Upper-right: linear representation of a NMDAR subunit peptide sequence-domain structure. Lower-right: Aligned peptide sequences of rat NMDARs subunits representing membrane domain 4 (M4) and the C-terminal region adjacent to M4. Amino acids in bold (GluN1, green; GluN2A-D, red), as indicated by a black arrowhead, is the site after which the CTD is deleted. (**B**) Representative two-electrode voltage clamp recordings displaying UBP684 (50 μM) induced potentiation of L-glutamate / glycine (10 μM each) - evoked currents at GluN1/GluN2A and GluN1/GluN2C NMDARs with ($GluN^{WT}$) or without ($GluN^{\Delta CTD}$) their CTD expressed in *Xenopus laevis* oocytes. Horizontal bars above traces show drug application. Horizontal scale bars indicate time (s) and vertical bars indicate current (nA). (**C**) Histogram showing average potentiation by UBP684 at GluN1/GluN2 receptors ($GluN2^{WT}$, black bars, n = 11 – 23 oocytes) and GluN1/CTD-deleted GluN2A-D receptors ($GluN2^{\Delta CTD}$, red bars, n = 13 – 28 oocytes). Negative values of % potentiation indicate inhibition. Data represent mean ± s.e.m. *$p < 0.05$, ***$p < 0.001$, ****$p < 0.0001$ (2-way ANOVA) (**D**) Mean potentiation of agonist-induced responses by UBP684 at receptors containing GluN2A-D subunits co-expressed with wild-type ($GluN1^{WT}$, black bars, n = 6 – 22 oocytes) or CTD-deleted GluN1 subunits ($GluN1^{\Delta CTD}$, green bars, n = 6 – 17 oocytes). Data represent mean ± s.e.m. ***$p < 0.001$, ****$p < 0.0001$ (2-way ANOVA). (**E**) Mean potentiation of agonist-induced responses by UBP684 at receptors containing GluN1 with full-length GluN2C ($GluN2C^{WT}$, black bars, n = 17 oocytes) or with GluN2C subunits with their CTD-truncated at 3 different sites (GluN2C-

855K^{STOP}, dark red bars, n = 9 oocytes, GluN2C-994L^{STOP}, red bars, n = 6 oocytes, GluN2C-1120C^{STOP}, light red bars, n = 6 oocytes). Data represent mean ± s.e.m. **** $p < 0.0001$ (Compared to 855K^{STOP}; One-way ANOVA).

Figure 2. Effect of NMDAR C-terminals on allosteric modulation by pregnenolone sulphate (PS)

(**A**) Representative current traces from two-electrode voltage clamp recordings showing the potentiation of responses to 10 μM glutamate /10 μM glycine by PS (100 μM) at recombinant GluN1/GluN2A and GluN1/GluN2C NMDARs with (GluN^{WT}) or without their CTDs (GluN$^{\Delta CTD}$). Horizontal bars above traces show the corresponding drug application protocol. Scale bars: horizontal, time in sec; vertical, current in nA. (**B**) Average potentiation of agonist-induced responses by PS at GluN1/GluN2 receptors (GluN2^{WT}, black bars) and at receptors with GluN2 CTD-deleted (GluN2$^{\Delta CTD}$, red bars) subunits (n = 4 - 25 oocytes). Negative values indicate % inhibition of agonist-evoked response. (**C**) Mean potentiation by PS of agonist-induced responses at receptors containing GluN2A-D subunits and GluN1^{WT} (black bars) or GluN1$^{\Delta CTD}$ subunits (green bars) (n = 6 – 24 oocytes). Negative values indicate % inhibition of agonist-evoked response. Data represent mean ± s.e.m. *$p < 0.05$, ****$p < 0.0001$ (2-way ANOVA). (**D**) Mean potentiation of agonist-induced responses by PS at GluN1/GluN2C (GluN2C^{WT}, black bars, n = 10 oocytes) or receptors with GluN2C truncated at 3 different CTD sites (GluN2C-855K^{STOP}, dark red bars, n = 5 oocytes, GluN2C-994L^{STOP}, red bars, n = 5 oocytes, GluN2C-1120C^{STOP}, light red bars, n = 5 oocytes). Data represent mean ± s.e.m. *$p < 0.05$, ** $P < 0.01$ (Compared to 855K^{STOP}; One-way ANOVA).

Figure 3. Impact of GluN2A-D C-terminals on PS activity/potency

Concentration-response for PS modulation of agonist responses (10 μM L-glutamate /10 μM glycine) at GluN1/GluN2(A-D)^{WT} receptors (black) and GluN1/GluN2(A-D)$^{\Delta CTD}$ receptors (red) expressed in X*enopus* oocytes. Data represent mean ± s.e.m., n = 5 – 8 oocytes each.

Figure 4. Effect of C-terminal deletion on potentiation by other PAMs

(A – D) Left panel: Average % potentiation of L-glutamate / glycine (10 μM each) evoked currents by mechanistically-distinct NMDAR PAMs. Right panel: Representative current traces showing the activity of the PAMs without (black trace) and with CTD deletions (red trace) from GluN2 subunits as indicated. **(A)** GluN2A-selective PAM GNE-8324 (30 μM) at GluN1/GluN2A (GluN2A^{WT}, black bar, n = 26 oocytes) and GluN1/GluN2A$^{\Delta CTD}$ (GluN2A$^{\Delta CTD}$ red bar, n = 23 oocytes) receptors. Negative values indicate % inhibition. ****p < 0.0001 (unpaired t- test). (**B**) Potentiation by the GluN2B-specific PAM spermine (100 μM) at GluN1/GluN2B (GluN2B^{WT}, black bar, n = 5 oocytes) and GluN1/GluN2B$^{\Delta CTD}$ (red bar, n = 7 oocytes) receptors. ***p < 0.001 (unpaired t- test). (**C**) Potentiation by GluN2C-specific PAM PYD-106 (30 μM) at GluN1/GluN2C (GluN2C^{WT}, black bar, n = 13 oocytes) and GluN1/GluN2C$^{\Delta CTD}$ (red bar, n = 9 oocytes) receptors. ****p < 0.0001 (unpaired t- test). (**D**) Potentiation by GluN2C/2D-specific PAM CIQ (10 μM) at GluN1/GluN2(C-D)^{WT} (black, n = 7 - 17 oocytes) and GluN1/GluN2(C-D)$^{\Delta CTD}$ receptors (red, n = 10 – 17 oocytes). (**E**) Mean potentiation of agonist-induced responses by 30 μM GNE-8324 at receptors containing GluN2A subunits co-expressed with wild-type GluN1 (GluN1^{WT}, black bars, n = 7 oocytes) or GluN1 CTD-deleted (GluN1$^{\Delta CTD}$, green bars, n = 5 oocytes) subunits. Data

represent mean ± s.e.m. (**F**) Mean potentiation of agonist-induced responses by CIQ (10 μM) at GluN1/GluN2D^{WT} (black bars, n = 18 oocytes) or GluN1/GluN2D$^{\Delta CTD}$ (green bars) receptors **(G)** Mean potentiation of agonist-induced responses by PYD-106 (30 μM) at receptors containing GluN1 subunits co-expressed with GluN2C^{WT} (black bars, n = 18 oocytes) or GluN2C subunits CTD-truncated at 3 different sites (GluN2C-855K^{STOP}, dark red bars, n = 9 oocytes, GluN2C-994L^{STOP}, red bars, n = 6 oocytes, GluN2C-1120C^{STOP}, light red bars, n = 5 oocytes). Data represent mean ± s.e.m. **** $p < 0.0001$ (one-way ANOVA).

Figure 5. Effect of C-terminal deletion on inhibition by different classes of NAMs

Inhibition of agonist-evoked (10 μM L-glutamate / 10 μM glycine) currents by different NAMs at GluN1/GluN2 receptors that have full-length CTDs (GluN^{WT}, black bars) or receptors containing GluN1 with GluN2$^{\Delta CTD}$ subunits (red bars), or GluN2 with GluN1$^{\Delta CTD}$ subunits (green bars). **(A)** 100 μM Pregnanolone sulphate (PAS) inhibition at GluN1/GluN2 (n = 4 - 8 oocytes) and GluN1/GluN2$^{\Delta CTD}$ (n = 4 oocytes) receptors. (**B**) Inhibition of agonist-evoked currents by 30 μM UBP792 at GluN1/GluN2^{WT} (n = 4 - 5 oocytes) and GluN1/GluN2$^{\Delta CTD}$ (n = 4-7 oocytes) receptors. (**C**) Inhibition by DQP-1105 (50 μM at GluN2A$^{WT/\Delta CTD}$ and 10 μM at GluN2C-D$^{WT/\Delta CTD}$) at GluN1/GluN2^{WT} (n = 5-13 oocytes) and GluN1/GluN2$^{\Delta CTD}$ (n = 5-10 oocytes) receptors. (**D-F**) Mean inhibition by GluN2A-specific NAMs (**D**) TCN-201 (10 μM) (**E**) MPX-004 (10 μM) and (**F**) MPX-007 (10 μM) at GluN1/GluN2A^{WT} (black bars, n = 3 - 7 oocytes) and GluN1/GluN2A$^{\Delta CTD}$ (n = 3 - 8 oocytes) receptors. (**G-I**) Average inhibition by (**G**) PAS (100 μM), (**H**) DQP-1105 (50 μM) and (**I**) TCN-201 (10 μM) at receptors containing GluN2A co-expressed with GluN1^{WT} (n = 7 - 9 oocytes) or GluN1$^{\Delta CTD}$ subunits (n = 4 – 5 oocytes). Values represent

mean ± s.e.m., *p < 0.05, **p < 0.01, ***p < 0.001, ****p < 0.0001, two-way ANOVA (A-C) or unpaired t-test (D-I).

Figure 6. Effect of intracellular calcium chelation and PLC inhibition on UBP684 and PS activity

(**A-D)** Average UBP684 potentiation of agonist-induced NMDAR responses from oocytes un-injected (open bar), water-injected (50 nL, black bar) or EGTA-injected (5 mM, 50 nL, blue bar) and expressing (**A**) GluN1/GluN2A, (**B**) GluN1/GluN2B, (**C**) GluN1/GluN2C or **(D)** GluN1/GluN2D receptors. Data represent mean ± s.e.m., n = 6 -19 oocytes. ***p<0.001, ****p<0.0001 (one-way ANOVA). (**E-H**) PS potentiation of control (open bar), water-injected (black) or EGTA-injected (blue) oocytes expressing **(E)** GluN1/GluN2A, (**F**) GluN1/GluN2B, (**G**) GluN1/GluN2C or **(H)** GluN1/GluN2D receptors. **(I, J)** Potentiation of agonist-evoked NMDAR currents by UBP684 (50 μM) (**I**) or PS (100 μM) (**J**) after oocytes were incubated with PLC inhibitor U73122 (blue bars, 20 μM / 30 min) or control media (black bars). Data represent mean ± s.e.m. (n = 4 - 15 oocytes). ****p<0.0001 (2-way ANOVA).

Figure 7. Effect of PKC and PKA activation on UBP684 and PS activity

(**A**) GluN1/GluN2A and GluN1/GluN2B receptor responses to 10 μM L-glutamate / 10 μM glycine were enhanced by prior incubation with 10 μM FSK and 1 mM IBMX for 10 minutes to activate PKA, n = 4 - 5 oocytes. **p<0.010 (unpaired t-test). (**B, C**) Potentiation by 50 μM UBP684 (**B**) and 100 μM PS (**C**) of GluN1/GluN2A and GluN1/GluN2B receptor responses before (black) or after (blue) PKA activation by FSK / IBMX, n = 4 - 6 oocytes. (**D**) PKC activation (2

μM PMA, 10 minutes) enhanced agonist-induced GluN1/GluN2A and GluN1/GluN2B receptor responses (n = 4 - 9 oocytes). (**E, F**) Potentiation of receptors containing GluN2A and GluN2B subunits by (**E**) 50 μM UBP684 (n = 9 - 11 oocytes) and (**F**) 100 μM PS (n = 3 - 9 oocytes) before (black) or after (blue) PMA incubation. **p<0.01 (2-way ANOVA). (**G, H**) Effect of C-terminal deletion on potentiation by (**G**) 50 μM UBP684 (n = 3 - 5 oocytes) and (**H**) 100 μM PS (n = 3 - 5 oocytes) after PMA incubation at GluN1/GluN2A$^{\Delta CTD}$ and GluN1/GluN2B$^{\Delta CTD}$ receptors. **p<0.01 (2-way ANOVA). (**I**) Potentiation of agonist-induced responses by UBP684 (50 μM) or PS (100 μM) 30 minutes after alkaline phosphatase (blue) or water (black) injection at oocytes expressing GluN1/GluN2B receptors (n = 4 - 9 oocytes). *p<0.05 (2-way ANOVA).

Figure 8. UBP684, but not PS, modulates the FRET signal between GluN1 CTDs.

A. Representative images of rat hippocampal neurons expressing GluN1-GFP, GluN2A and GluN1-mCherry before and 10-15min after application of UBP684 (75 μM) or PS (75 μM). Pseudocolor scale indicates GFP lifetime at each pixel; scale bar is 5μm. Arrows indicate spines with obvious lifetime increases. B. UBP684 induced a significant increase of GluN1-GFP fluorescence lifetime, indicating a reduction in FRET between GluN1 CTDs. PS did not affect the NMDAR conformation as measured by this assay. N>17 neurons, >550 spines per condition, ***p<0.001 (unpaired t-test).

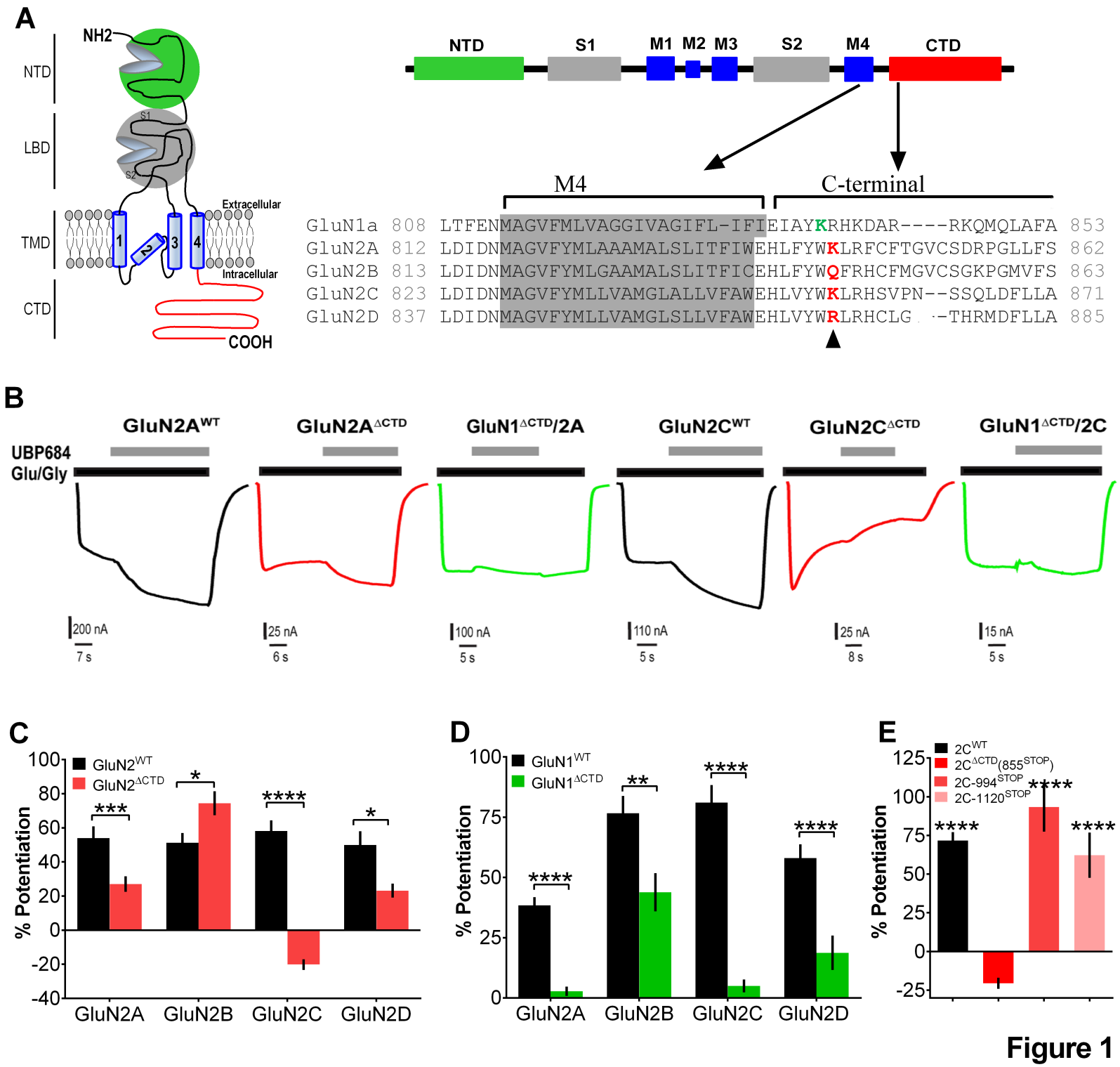
A
NH2
NTD
LBD
TMD
CTD
COOH
Extracellular
Intracellular
S1
S2
1
2
3
4
NTD
S1
M1
M2
M3
S2
M4
CTD
M4
C-terminal
GluN1a 808 LTFENMAGVFMLVAGGIVAGIFL-IFIEIAYKRHKDAR----RKQMQLAFA 853
GluN2A 812 LDIDNMAGVFYMLAAAMALSLITFIWEHLFYWKLRFCFTGVCSDRPGLLFS 862
GluN2B 813 LDIDNMAGVFYMLGAAMALSLITFICEHLFYWQFRHCFMGVCSGKPGMVFS 863
GluN2C 823 LDIDNMAGVFYMLLVAMGLALLVFAWEHLVYWKLRHSVPN--SSQLDFLLA 871
GluN2D 837 LDIDNMAGVFYMLLVAMGLSLLVFAWEHLVYWRLRHCLG--THRMDFLLA 885
B
GluN2A^WT
GluN2A^ΔCTD
GluN1^ΔCTD/2A
GluN2C^WT
GluN2C^ΔCTD
GluN1^ΔCTD/2C
UBP684
Glu/Gly
200 nA
7 s
25 nA
6 s
100 nA
5 s
110 nA
5 s
25 nA
8 s
15 nA
5 s
C
% Potentiation
GluN2^WT
GluN2^ΔCTD
GluN2A
GluN2B
GluN2C
GluN2D
D
% Potentiation
GluN1^WT
GluN1^ΔCTD
GluN2A
GluN2B
GluN2C
GluN2D
E
% Potentiation
2C^WT
2C^ΔCTD(855^STOP)
2C-994^STOP
2C-1120^STOP

Figure 1

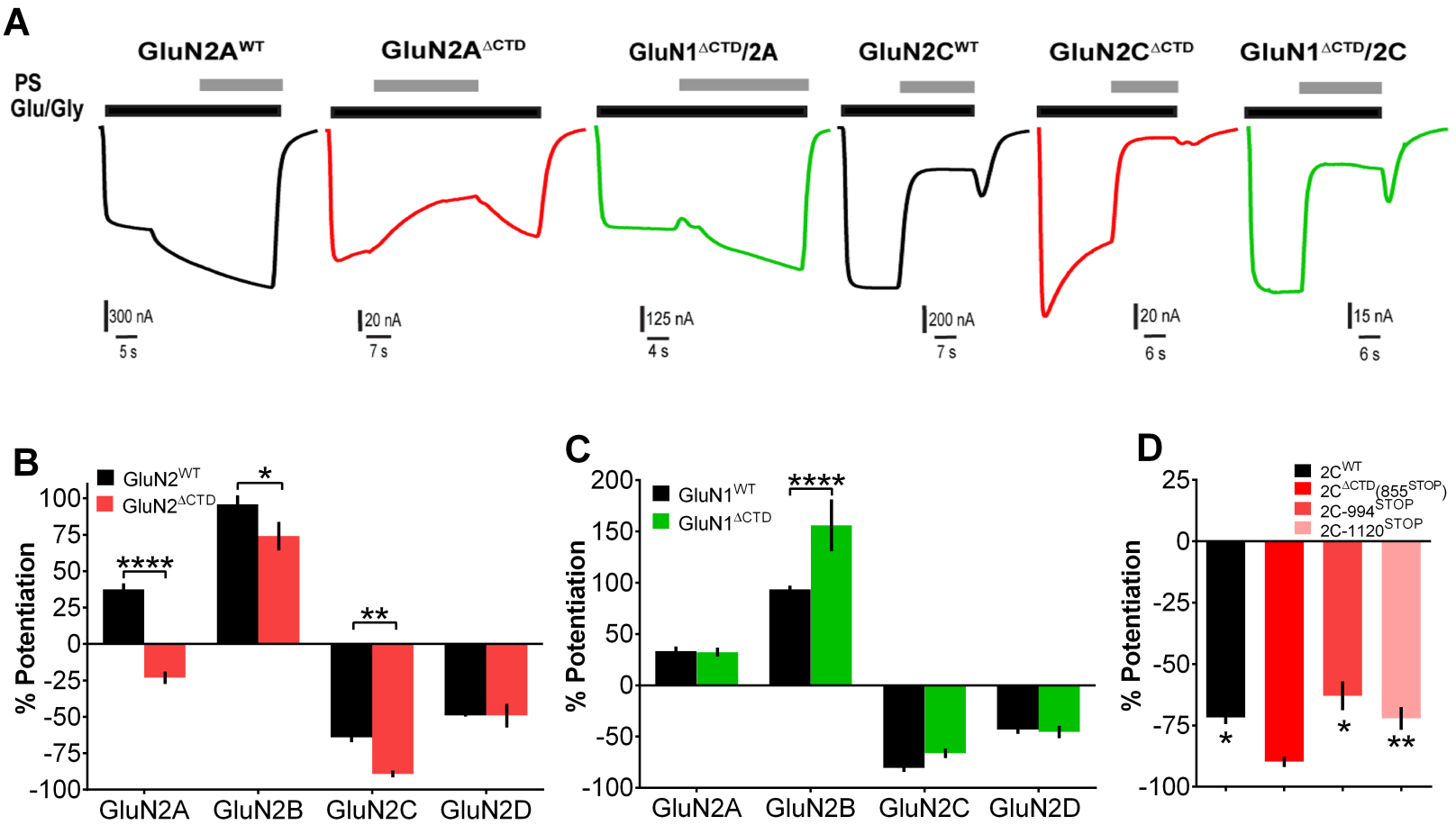
A
GluN2A^WT
GluN2A^ΔCTD
GluN1^ΔCTD/2A
GluN2C^WT
GluN2C^ΔCTD
GluN1^ΔCTD/2C
PS
Glu/Gly
300 nA
5 s
20 nA
7 s
125 nA
4 s
200 nA
7 s
20 nA
6 s
15 nA
6 s
B
GluN2^WT
GluN2^ΔCTD
% Potentiation
GluN2A
GluN2B
GluN2C
GluN2D
C
GluN1^WT
GluN1^ΔCTD
% Potentiation
GluN2A
GluN2B
GluN2C
GluN2D
D
2C^WT
2C^ΔCTD(855^STOP)
2C-994^STOP
2C-1120^STOP
% Potentiation

Figure 2

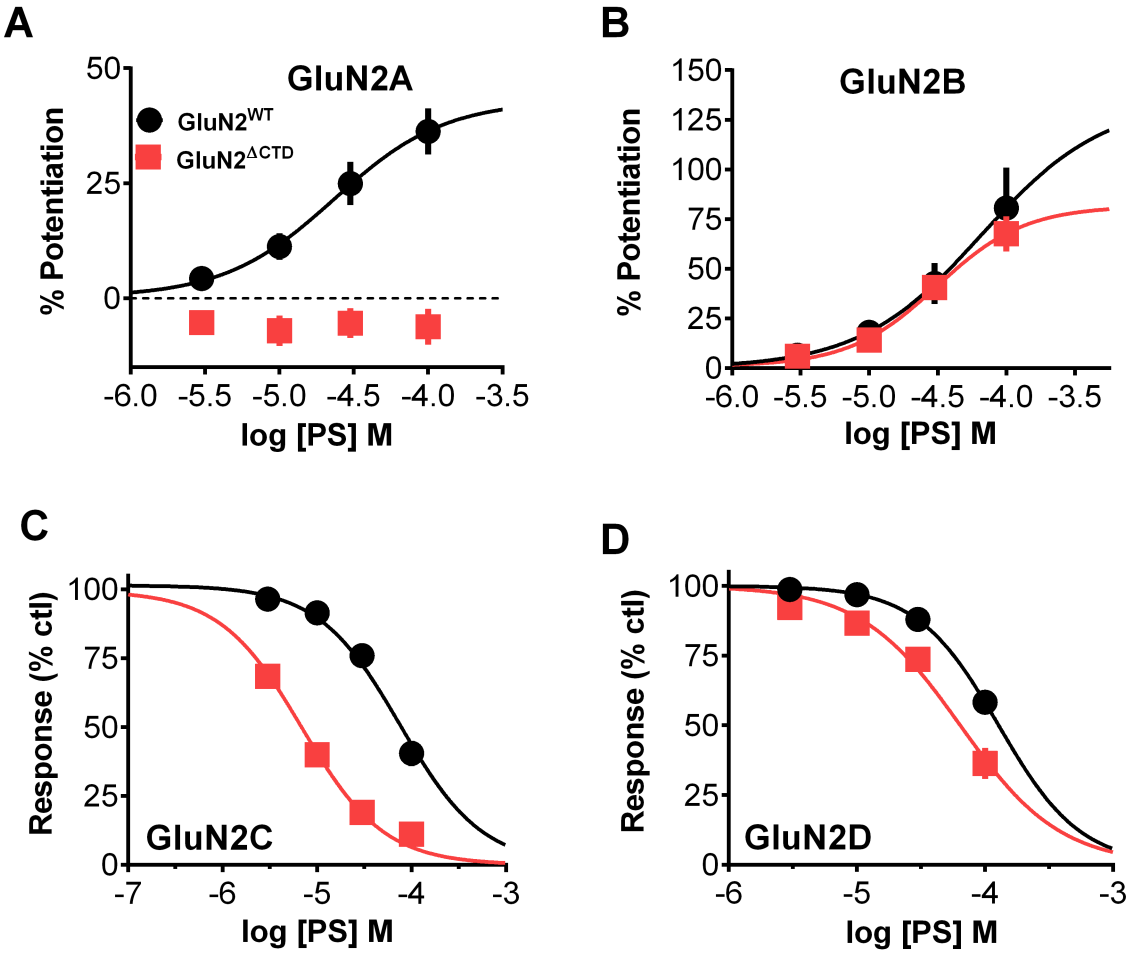
A
GluN2A
GluN2WT
GluN2ΔCTD
% Potentiation
50
25
0
-6.0 -5.5 -5.0 -4.5 -4.0 -3.5
log [PS] M
B
GluN2B
% Potentiation
150
125
100
75
50
25
0
-6.0 -5.5 -5.0 -4.5 -4.0 -3.5
log [PS] M
C
Response (% ctl)
100
75
50
25
0
GluN2C
-7 -6 -5 -4 -3
log [PS] M
D
Response (% ctl)
100
75
50
25
0
GluN2D
-6 -5 -4 -3
log [PS] M

Figure 3

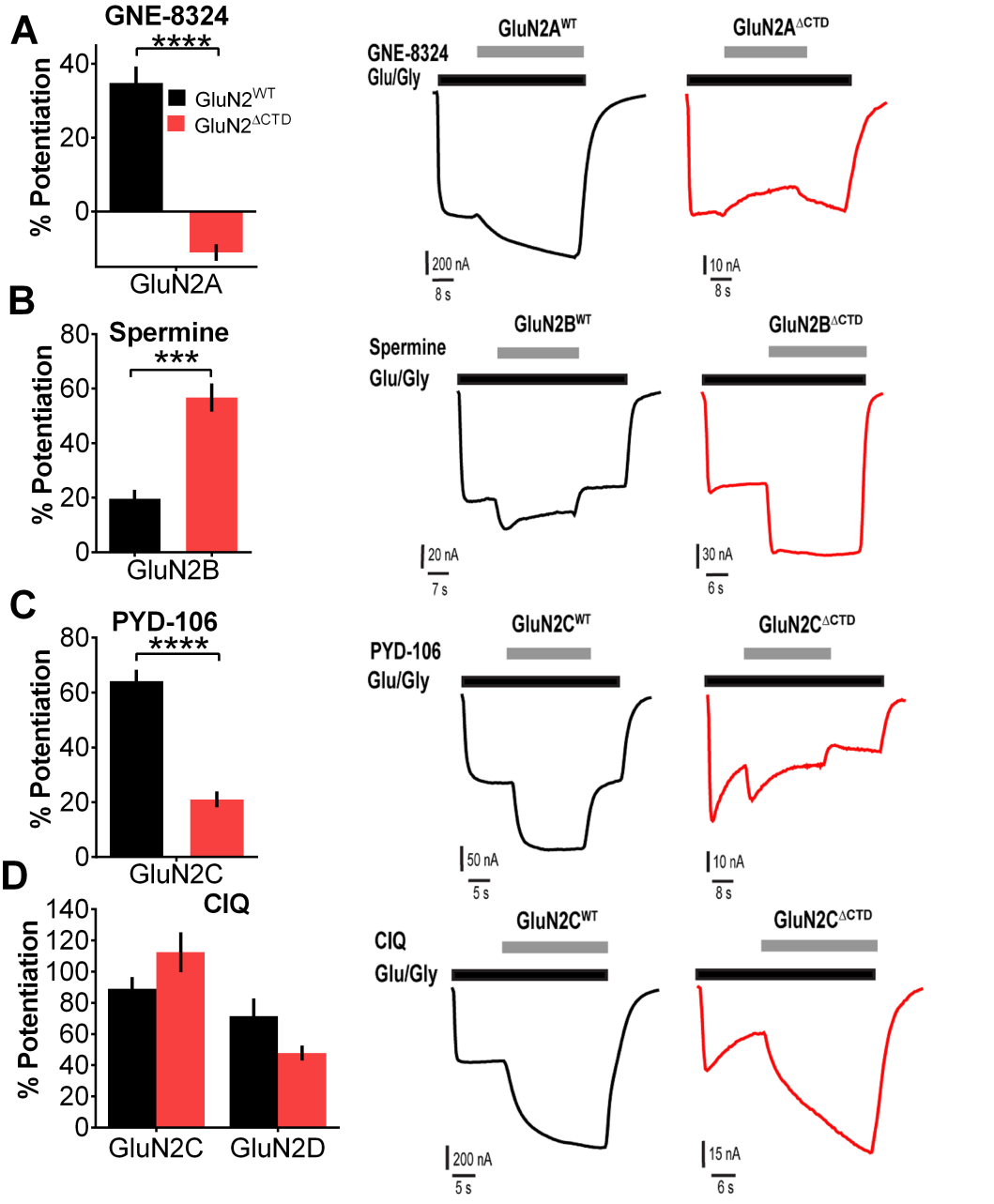
A
GNE-8324
****
% Potentiation
40
20
0
GluN2^WT
GluN2^ΔCTD
GluN2A
B
Spermine
***
% Potentiation
80
60
40
20
0
GluN2B
C
PYD-106
****
% Potentiation
80
60
40
20
0
GluN2C
D
CIQ
% Potentiation
140
120
100
80
60
40
20
0
GluN2C
GluN2D
GluN2A^WT
GluN2A^ΔCTD
GNE-8324
Glu/Gly
200 nA
8 s
10 nA
8 s
GluN2B^WT
GluN2B^ΔCTD
Spermine
Glu/Gly
20 nA
7 s
30 nA
6 s
GluN2C^WT
GluN2C^ΔCTD
PYD-106
Glu/Gly
50 nA
5 s
10 nA
8 s
GluN2C^WT
GluN2C^ΔCTD
CIQ
Glu/Gly
200 nA
5 s
15 nA
6 s
E
GNE-8324
% Potentiation
40
30
20
10
0
GluN1^WT
GluN1^ΔCTD
GluN2A
F
CIQ
***
40
30
20
10
0
GluN2D
G
PYD-106
****
****
% Potentiation
100
80
60
40
20
0
2C^WT
2C^ΔCTD(855^STOP)
2C-994^STOP
2C-1120^STOP

Figure 4

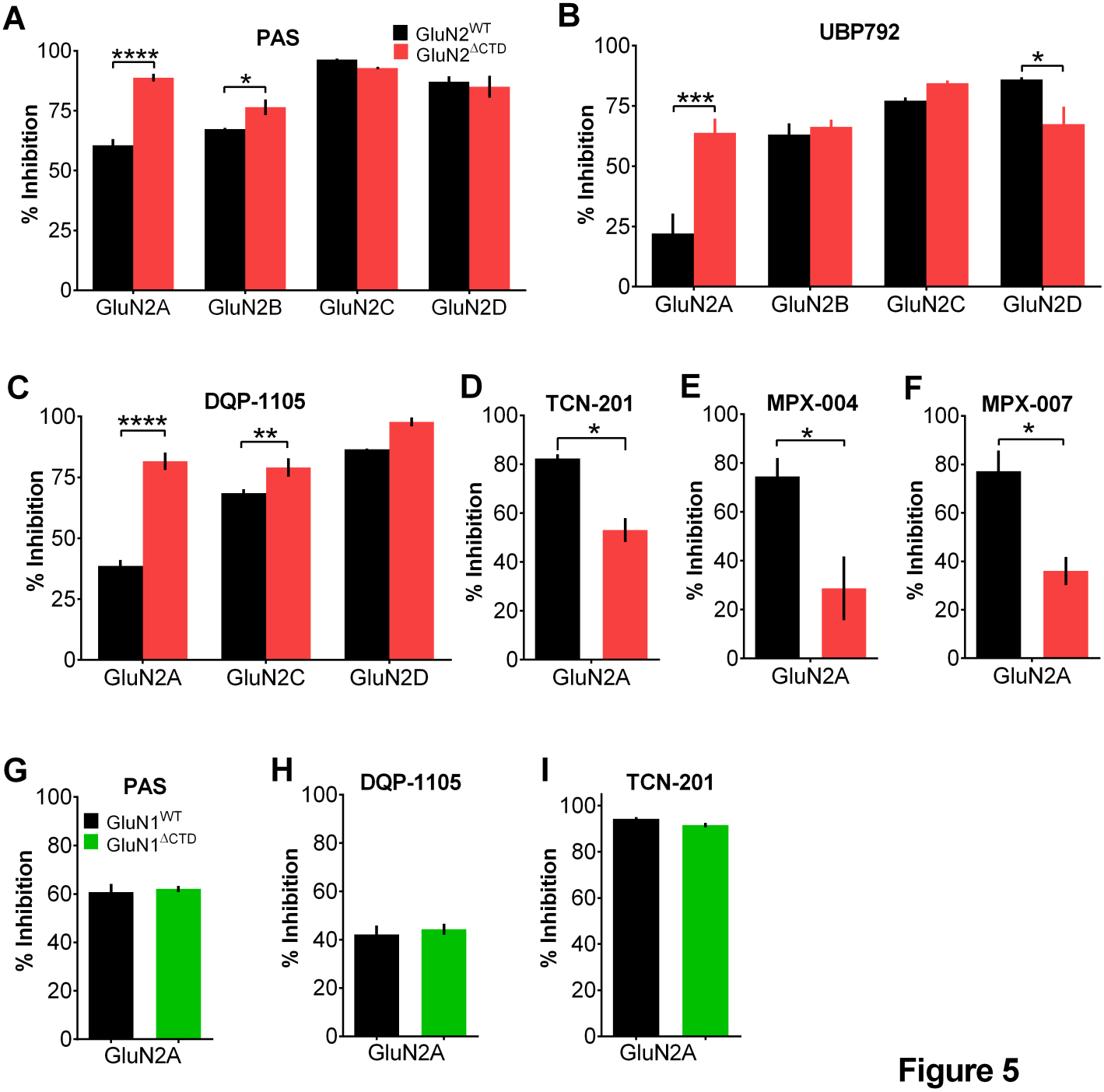
A
PAS
GluN2WT
GluN2ΔCTD
% Inhibition
GluN2A
GluN2B
GluN2C
GluN2D
B
UBP792
C
DQP-1105
D
TCN-201
E
MPX-004
F
MPX-007
G
PAS
GluN1WT
GluN1ΔCTD
H
DQP-1105
I
TCN-201

Figure 5

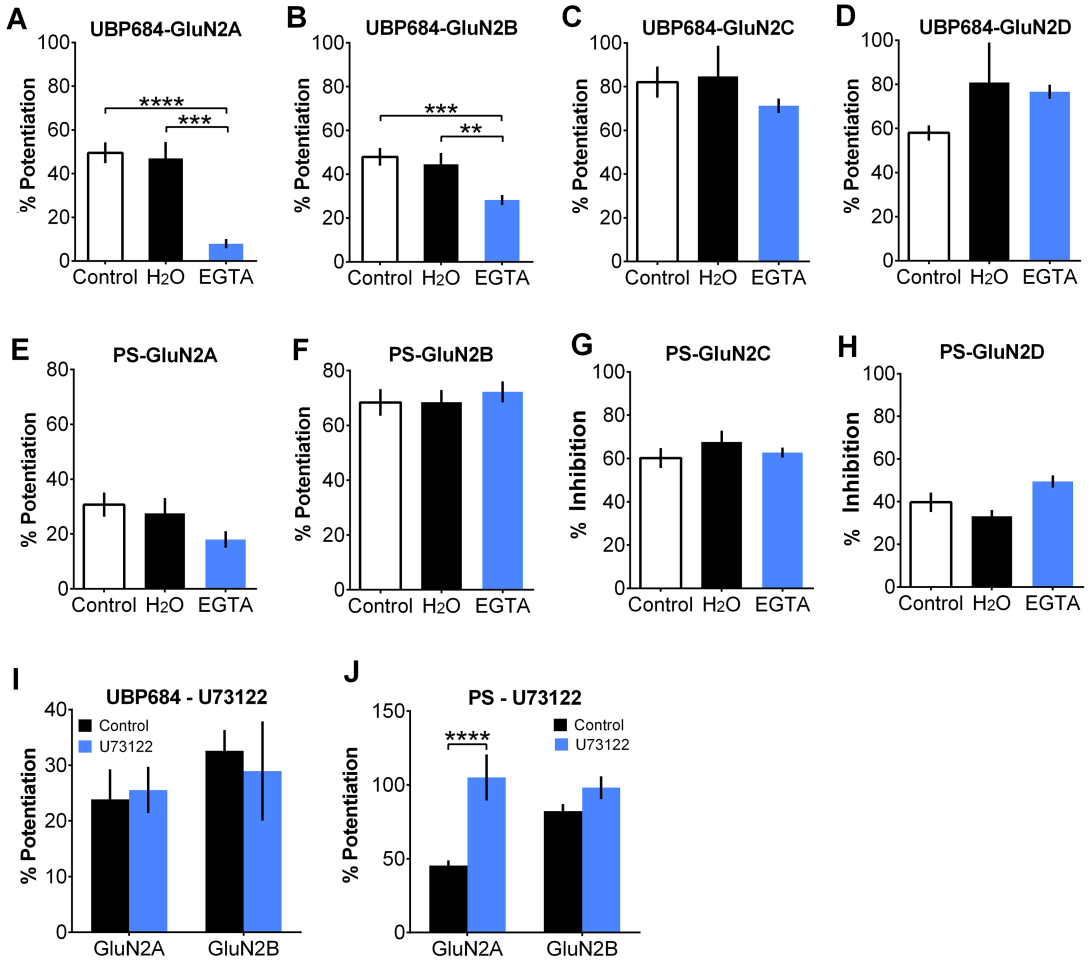
A
UBP684-GluN2A
% Potentiation
Control
H2O
EGTA
****
***
B
UBP684-GluN2B
***
**
C
UBP684-GluN2C
D
UBP684-GluN2D
E
PS-GluN2A
F
PS-GluN2B
G
PS-GluN2C
% Inhibition
H
PS-GluN2D
I
UBP684 - U73122
Control
U73122
GluN2A
GluN2B
J
PS - U73122

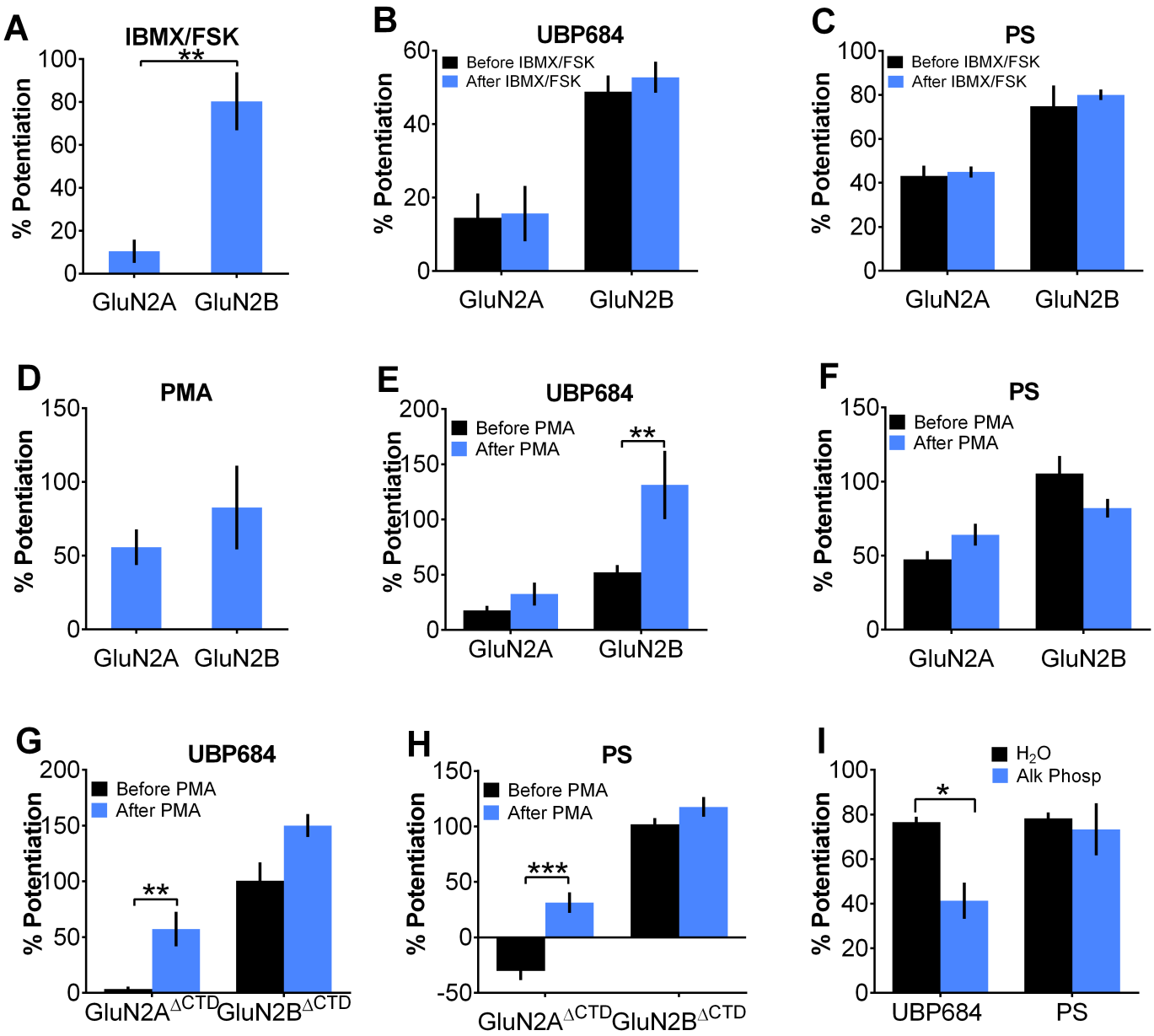
A
IBMX/FSK
% Potentiation
100
80
60
40
20
0
**
GluN2A
GluN2B
B
UBP684
Before IBMX/FSK
After IBMX/FSK
% Potentiation
60
40
20
0
GluN2A
GluN2B
C
PS
Before IBMX/FSK
After IBMX/FSK
% Potentiation
100
80
60
40
20
0
GluN2A
GluN2B
D
PMA
% Potentiation
150
100
50
0
GluN2A
GluN2B
E
UBP684
Before PMA
After PMA
% Potentiation
200
150
100
50
0
**
GluN2A
GluN2B
F
PS
Before PMA
After PMA
% Potentiation
150
100
50
0
GluN2A
GluN2B
G
UBP684
Before PMA
After PMA
% Potentiation
200
150
100
50
0
**
GluN2A^ΔCTD
GluN2B^ΔCTD
H
PS
Before PMA
After PMA
% Potentiation
150
100
50
0
-50
***
GluN2A^ΔCTD
GluN2B^ΔCTD
I
H2O
Alk Phosp
% Potentiation
100
80
60
40
20
0
*
UBP684
PS

Figure 7

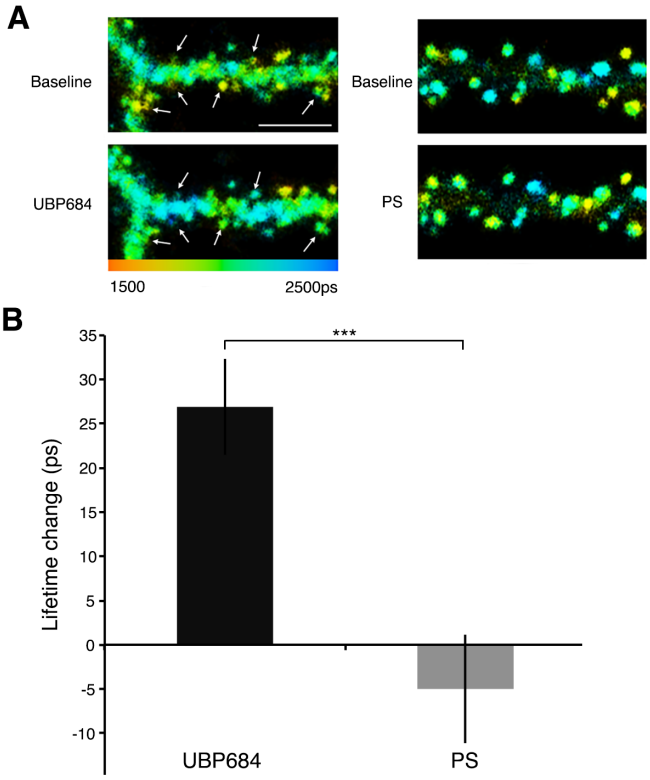
A
Baseline
Baseline
UBP684
PS
1500
2500ps
B
***
Lifetime change (ps)
35
30
25
20
15
10
5
0
-5
-10
UBP684
PS

Figure 8